DEVELOPMENT OF GELATIN METHACRYLAMIDE - HYDROXYPROPYL METHACRYLATE BASED BIOINK

Ms. NITHUSHA K.
REG NO: 2017/MPHIL/01

A THESIS SUBMITTED FOR THE DEGREE OF

MASTER OF PHILOSOPHY

SREE CHITRA TIRUNAL INSTITUTE FOR MEDICAL SCIENCES AND TECHNOLOGY
THIRUVANANTHAPURAM – 695 012

JULY 2018

DECLARATION

I, **NITHUSHA K**, hereby certify that I had personally carried out the work depicted in the dissertation entitled, ***"Development of Gelatin methacrylamide-Hydroxypropyl methacrylate based bioink",*** under the direct supervision of Dr.V.Kalliyana Krishnan, Scientist G (Senior Grade), Scientist-in-Charge, Division of Dental Products and Head, Department of Biomaterials Science & Technology, Biomedical Technology Wing, Sree Chitra Tirunal Institute for Medical Sciences & Technology, Thiruvananthapuram, Kerala, India except where due acknowledgment has been made in the text. No part of the thesis has been submitted for the award of any other degree or diploma prior to this date.

Thiruvananthapuram — NITHUSHA K.

30-07-2018 — Reg.No: 2017/MPhil/01

SREE CHITRA TIRUNAL INSTITUTE FOR MEDICAL SCIENCES & TECHNOLOGY
BIOMEDICAL TECHNOLOGY WING, POOJAPPURA
THIRUVANANTHAPURAM – 695011, INDIA
(An Institute of National Importance under Govt. of India)
Phone-(91)0471-2520221 Fax-(91)0471-2341814 www.sctimst.ac.in

Dr. V. Kalliyana Krishnan
Scientist G (Senior Grade) & Scientist-In-Charge,
Division of Dental Products
Head, Department of Biomaterials Science & Technology,
BMT Wing, SCTIMST
email: kalyankv@sctimst.ac.in

This is to certify that **Ms. NITHUSHA K.** has fulfilled the requirements prescribed for the MPhil degree of the Sree Chitra Tirunal Institute for Medical Sciences and Technology, Thiruvananthapuram. The dissertation entitled, **"*Development of gelatin methacrylamide- hydroxypropyl methacrylate based bioink*"** was carried out under my direct supervision. No part of the thesis was submitted for the award of any degree or diploma prior to this date.

Thiruvananthapuram
Date: 30-07-2018

Dr. V. Kalliyana Krishnan
(Research Supervisor)

The dissertation entitled

"DEVELOPMENT OF GELATIN METHACRYLAMIDE-HYDROXYPROPYL METHACRYLATE BASED BIOINK"

Submitted by

Ms. NITHUSHA K.

for the degree of

Master of Philosophy

of

SREE CHITRA TIRUNAL INSTITUTE
FOR MEDICAL SCIENCES AND TECHNOLOGY
THIRUVANANTHAPURAM - 695011

is evaluated and approved by

…….	……..
Dr. V. Kalliyana Krishnan	Examiner's name and
(Research Supervisor)	Designation

Dedicated to

MY TEACHERS & MY FAMILY

ACKNOWLEDGEMENTS

It is with deep sense of gratitude, satisfaction and with the divine blessings of GOD ALMIGHTY that I submit this dissertation. I take this opportunity with much pleasure to thank all who contributed in many ways for the success of this study.

I have no words to express my deepest sense of gratitude and respect to my guide Dr. V Kalliyana Krishnan, Scientist G (Senior Grade) & Scientist-In -Charge, Division of Dental Products (DEP), BMT wing, SCTIMST who offered continuous advice, constant encouragement, inspiring discussions and valuable suggestions to do this work with confidence. He took significant efforts for the successful completion of this project. I would also like to thank Prof. Asha Kishore, Director of SCTIMST and Dr. Harikrishna Varma P.R, Head, BMT Wing, SCTIMST, for providing all the facilities to carry out my M.Phil.dissertation.

I am extremely grateful to Dr. Shiny Velayudhan, Scientist D, Division of Dental Products for her constant encouragement and support, valuable advice, kind cooperation, and extensive help extended throughout my work without which I would not have completed this project successfully.

I am thankful to Dr. V Kalliyana Krishnan (Dean of Academic Affairs), Dr. B. Santhosh Kumar (Deputy Registrar) and all members of academic division for their assistance.

I am grateful to Dr. Lissy K Krishnan, Scientist G & SIC, Thrombosis research unit (TRU), SCTIMST for providing me with facilities to carry out the biological part of the work.

I am indebted to Dr. A. Maya Nandkumar, Dr. Manoj Komath, and Dr. Francis Boniface Fernandez our course coordinators, for all the help extended to me. I am also thankful to all the faculty members of M.Phil.course work who took lot of pains to make our courses enriching and worthwhile.

I am grateful to Ms. Rashmi R, TRU for her kind cooperation and help for completing all the cell culture studies. The help from all other colleagues of TRU, Dr. Anugya Bhatt, and Ms. Anusree K.S, is acknowledged.

I am thankful to Dr. Naresh Kasoju, Division of Tissue Culture for his kind corporation for confocal analysis. I am thankful to Ms. Shilpa Ajit and Mr. Roopesh R Pai for helping with 3D printing of the bioink.

I am thankful to Dr. Sunitha Prem Victor, and Dr. Sasikala, Division of Polymer Analysis for recording the FTIR spectra.

I wish to express my thanks to Dr.Luxmi Varma and her colleagues of National Institute of Interdisciplinary Research (NIIST), Trivandrum for providing the NMR spectra and the rheological data.

I am thankful to Dr. Lizymol P.P. and all my labmates at Dental Products Laboratory for their friendship and help. I whole heartedly thank Dr. D.R.Deepu, Ms. M. Aysha Shafna and Ms. Bridget Jayatha, for their timely valuable advices, moral support and training me in many techniques. I extend my sincere thanks to Ms. Dhanya G.R, Ms. Vibha C, and Ms. Resmi R for their friendly support and help in various lab works. I extend my thanks to all my friends of the M.Phil. 2017-2018 batch for their friendship, cheerful times and for the ever memorable days in this campus. My friends and teachers are also acknowledged. Cooperation from staff of various administrative departments and library of the Institute is fondly remembered. Cordial attitude and support from labmates from other departments of our campus is acknowledged. I have no words to express my heartfelt gratitude and love to my family members who provided the most precious support. I am indebted to my parents, my sister and my husband for their endless support, encouragement, love and prayers.

GOD, ALMIGHTY I bow down in your presence for giving me strength, courage and for providing good health for completing this work

CONTENTS

LIST OF FIGURES

LIST OF TABLES

ABBREVIATIONS

3D printing	Three dimensional printing
DAPI	4',6-diamidino-2-phenylindole
DBB	Droplet-based Bioprinting
DMEM	Dulbecco's Modified Eagle's Medium
DMSO	Dimethyl Sulfoxide
EBB	Extrusion-based Bioprinting
ECM	Extracellular matrix
EtBr	Ethidium bromide
FBS	Foetal Bovine Serum
FDA	Fluorescein Diacetate
FTIR	Fourier transform Infrared Spectrophotometer
GelMA	Gelatin Methacrylamide
HPMA	Hydroxypropyl methacrylate
LBB	Laser-based Bioprinting
MA	Methacrylic anhydride
MicroCT	Micro-Computed Tomography
MSCs	Mesenchymal stem cells
MTT	3-(4, 5-Dimethylthiazol-2-yl)-2, 5-diphenyltetrazolium bromide
NMR	Nuclear Magnetic Resonance spectroscopy
PBS	Phosphate Buffered Saline
RT	Room Temperature
TCPS	Tissue Culture Polystyrene
TE	Tissue engineering
UTM	Universal Testing Machine

CHAPTER 1

INTRODUCTION

Three-dimensional printing was introduced by Charles W Hull in 1986. It is an additive manufacturing process to create 3D structures by adding layer by layer of materials such as plastic, metal, ceramic, polymers etc. 3D printing has an important role in tissue engineering. Tissue engineering (TE) deals with the restoration of injured and damaged tissues and organs. It involves biology, material science, engineering, surgery, and molecular technology. The aim of TE is to fabricate tissues and develop its biological functionality in order to overcome the problems like organ shortage. 3D bioprinting is a driving major innovation in this field. It enables the ease of fabrication of tissues and aim to solve these concerns. It utilizes the layer by layer deposition of materials known as bioink, to create tissue like structures.

Bioink is the backbone of three dimensional bioprinting. Bioinks are composed of mixture of cells, biomaterials and bio active molecules, in a liquid, pre-gel solution that creates the printed article into a 3D scaffold or onto a surface. The bioink solution is converted into gels using different processes such as thermal activation, photo activation, or using polymer crosslinkers while retaining the cell viability. Hydrogels are the class of materials used to prepare bioinks, which are highly hydrated and they can mimic or replace the native tissue environment. Hydrogels also promote and help in the development of tissues by providing a cell to cell attachment, cell migration and remolding of matrix. The final bioink construct is composed of cells and bioactive molecules incorporated within the hydrogels. For an ideal bioink, a hydrogel should

provide optimum mechanical strength, excellent printable character and good cell-scaffold interactions.

Gelatin based hydrogels are widely used as bioinks. Methacrylamide modified gelatin (GelMA) has recently gained increasing attention, mainly in the field of biomedical applications. GelMA can be used as tissue engineering scaffold material due to its excellent biocompatibility, mechanical properties as well as printability. Low concentration GelMA hydrogel possess excellent cell viability, however it suffers from poor processability during the printing process due to low viscosity, low gelation rate, and weak mechanical strength. Even though high concentration GelMA shows high printability, it suffers from decreased cell viability.

In this present study, GelMA was coupled with hydroxypropyl methacrylate (HPMA) through redox polymerization, to enhance the properties of GelMA and to study the feasibility of GelMA-HPMA combination for bioink application. This thesis gives an overview of different hydrogels used as a bioink and currently available GelMA based bioinks, its advantages and disadvantages (Chapter 2). The study proposes a hypothesis that the development of GelMA-HPMA based bioink using redox initiators may be a better alternative than developing the same polymer using UV photoinitiation especially because photoinitiation tends to damage the cells irreversibly during curing. Incorporation of HPMA is also expected to enhance the mechanical strength and printability characteristics of the hydrogel bioink.

In Chapter 3, the synthesis of hydrogels (GelMA-HPMA) at various concentrations, its characterization and biological studies are discussed. The characterization techniques such as FTIR, H^1 NMR, Mechanical strength, swelling analysis, viscosity, micro CT studies etc. have been described.

Chapter 4, explains about the results and discussion of the present study. Statistical analysis and calculation of standard deviation has been carried out wherever applicable.

Finally in Chapter 5, the summary, conclusion and future outlook of the work are presented. It gives a brief summary of the investigation along with the conclusion of the study and its future perspective.

CHAPTER 2

LITERATURE SURVEY

2.1. BIOPRINTING

The term bioprinting is defined as a "computer-aided transfer process for patterning and assembling living and nonliving materials with a prescribed layer-by-layer stacking organization in order to produce bio-engineered structures serving in regenerative medicine and other biological studies". This process involved mainly three steps: preprocessing, printing, and post processing. In the first step, preprocessing uses a computer-aided design technique to develop and design a blueprint of tissue or organ. In the second step, the blue printed design is printed using a bioprinter. Final process involved the tissue maturation and tissue regeneration of bioprinted construct in a bioreactor [Hospodiuk et al. 2017].

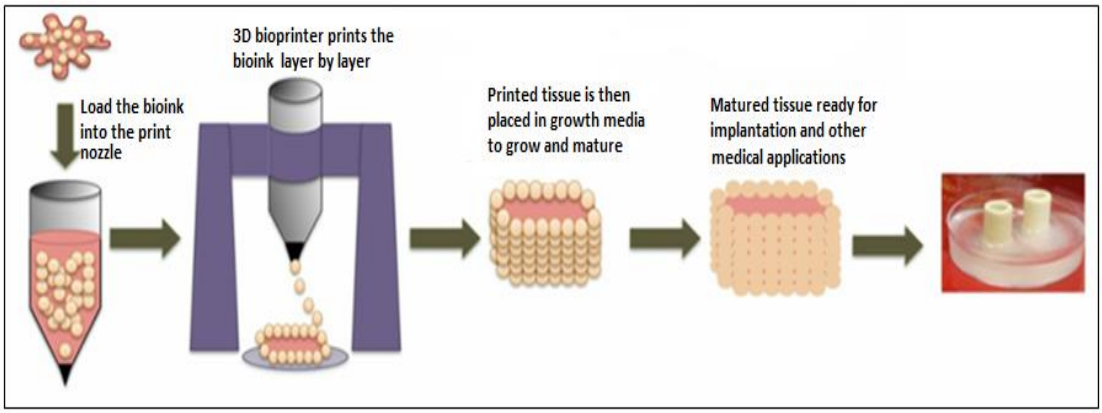

Figure 2. 1. Schematic representation of bioprinting *https://3dbioprinting.weebly.com/how-it-works.html*

2.2. BIOINK

Development of a biomaterial can be considered as one of the most difficult parts of bioprinting. A bioink is formed by the mixing of cells and biomaterials together to create a 3D tissue construct. The bioink required biological, physical and mechanical properties for cell viability and printability respectively [Hospodiuk et.al. 2017]. The bioink material development helps scientists to create complex biological constructs by manipulating the biological and biochemical environment along with the living cells. The sustained viability of cells during short cell culture, long cell culture, cell spreading and proliferation, interactions such as cell to cell and cell to the extracellular matrix (ECM), and bioprinted construct functionality are considered as the signs of success. Although, in the field of tissue engineering and regenerative medicine, a wide range of biomaterials have been developed [Furth et al., 2007], but the compatibility of many of them are not sufficient with existing bioprinting technologies. An ideal bioink material should have some important features like bioprintability, high mechanical integrity and stability, appropriate rate of biodegradability for regenerating tissue, insolubility in cell culture medium, non-immunogenicity and non-toxicity, and to promote cell adhesion ability. In addition, manufacturing and processing of bioink should be easy, inexpensive, and commercially obtainable. The designed shape, structural strength and integrity of a bioprinted construct are expected to keep and maintain their 3D architecture for a definite period of time *in vitro* as well as *in vivo*.

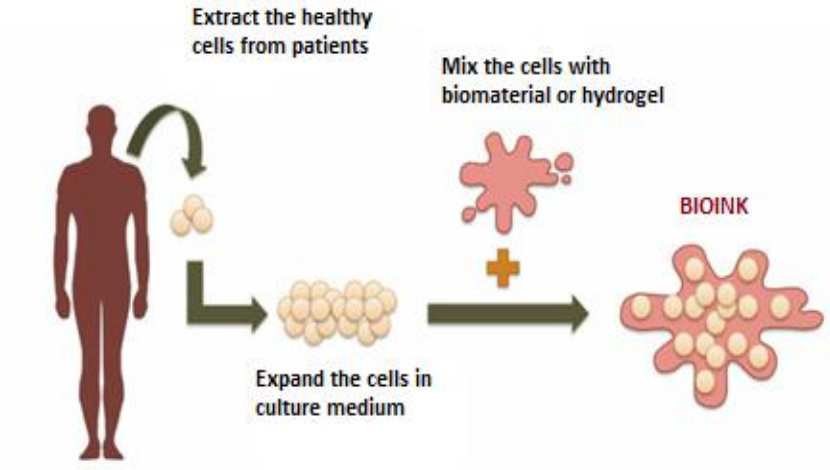

Figure 2. 2. Schematic representation of bioink *https://3dbioprinting.weebly.com/how-it-works.html*

There are two type of bioink materials used in 3D bioprinting technique, the first category is scaffold based (i.e. hydrogels, micro-carriers and de-cellularized matrix components), and second one is scaffold-free (i.e., cell aggregates) bioink materials. In scaffold-based bioink, the 3D constructs are bioprinted by the cells loaded into the hydrogels or similar exogenous materials and Cell-loaded hydrogels allow cell proliferation and growth, and facilitate the tissue formation. In the second type of bioink, the exogenous biomaterial is not used for cell bioprinting and embryonic development mimicked by a scaffold-free process. The first form of cells are known as neo-tissues that are engineered for bioprinting processes and for the fabrication of larger-scale functional tissues the resulting neo-tissues are deposited in specific shape where they fused and developed [Hospodiuk *et al*. 2017].

2.3. HYDROGELS AS BIOINKS

2.3.1. Hydrogels (Scaffold-based Bioink Materials):

Hydrogels are referred as a class of crosslinked polymeric substances capable of absorbing and retaining large quantities of water. In tissue engineering, hydrogels are classified into two groups: naturally-derived hydrogels and synthetically-derived hydrogels. Gelatin, fibrin, collagen, chitosan, and alginate are the examples for naturally derived hydrogels. Pluronic® or polyethylene glycol (PEG) are the examples for synthetically derived hydrogels. On the basis of where they have been derived from, naturally-derived hydrogels can be again classified. Vertebrate derived hydrogels such as collagen, fibrin, and gelatin have characteristic signaling molecules for cell adhesion whereas hydrogels derived from other living organisms such as algae or sea weeds lack these signaling molecules. Alginate and agarose are the examples for such hydrogels [Gasperini et al., 2014; Lee and Mooney, 2012]. Drug delivery [Yang et al., 2011], contact lenses [White et al., 2011] and wound dressings [Kamoun et al., 2015] are the applications of hydrogels used in biofabrication and tissue engineering. If hydrogels have numerous essential features of the native ECM components, they are capable to mimic the native tissue environment [Tibbitt and Anseth, 2009]. In an ideal 3D, an extremely hydrated environment, while having ECM-like properties will allow cell encapsulation; however there are some limitations for both natural and synthetic

polymer hydrogels. Weak mechanical properties of natural hydrogels limits their use in many applications while lack of key components such as bioactive molecules for cell adhesion or migration are the limitations of synthetic hydrogels [Zhu and Marchant, 2011]. Essential hydration level of hydrogels influence's its biocompatibility. In an aqueous medium, a hydrogel can absorb up to thousand times their actual weight without dissolving in it [Ahmed, 2013], making them a perfect cell encapsulation material. Hydrogels are smart materials for construction of tissue due to their high oxygen permeability, nutrients and other water-soluble compounds [Thomas et al., 2009; Zhu and Marchant, 2011]. Cells are normally seeded on the surface of scaffolds in the case of polymeric scaffolds used for tissue engineering, and the embedded cells getting a pleasant environment provided by the hydrogels, so inside the three dimensional area cells can migrate in any direction and through the porous flexible network it can interconnect with each other [Benedikt et al., 2000; Drury and Mooney, 2003; Rajan et al., 2006; Yamamoto et al., 2010]. Individual features of natural and synthetic hydrogels cannot be clearly specified; but, naturally derived hydrogels are cyto-compatible hence they are used in tissue engineering and bioapplications. But synthetic hydrogels have lack of biofuctionality [Hospodiuk et al. 2017].

In bioprinting, bioink materials were made up of hydrogels or it acts as a cell delivery vehicles. Fibroblasts, chondrocytes, hepatocytes, smooth muscle cells, adipocytes, and stem cells are the different type of cells which are viable inside the hydrogel when they are encapsulated in it. The various shape of a hydrogels, which are incorporated with cells were successively secure by gelation in bioprinting. The crosslinking reaction carried out by a physical or chemical or physiochemical processes is known as gelation. The reversible interaction takes place in physical crosslinking, and the meshes of high molecular polymer chains, ionic interactions and hydrogen bridges are the factors that affecting physical crosslinking. Growth factors, living cells like biological systems are compatible with this types of crosslinking. The interaction with anionic groups of alginate (COO) with divalent metal ions (Ca2þ) carried out ionotropic gelation is an example for physical crosslinking. On cooling the warm carrageenan solution will undergo helical aggregation and form a gel is another example for physical crosslinking. The main limitation of crosslinking reaction is poor mechanical properties. Hence incorporation of crosslinking agent or post processing

crosslinking is required to avoid this problem. Compared to physical crosslinking, chemical crosslinking has relatively high mechanical stability to the construct due to the formation of new covalent bond in it. Natural and synthetic polymers can be crosslinked by aldehyde crosslinkers and the reaction carried out in their -OH, -COOH, and -NH_2, functional groups. Glutaraldehyde, adipic acid dihydrazide are the aldehyde crosslinkers mainly used for this kind of reactions. In some cases, the embedded cells may be affected by the exposure of construct due to the irradiation existing in this kind of crosslinking. Encapsulated cells are difficult to migrate or mobile in the formed 3D mesh networks due to their small size than cells. To allow the migration and proliferation of cells it is achieved by incorporating degradation sites in hydrogels. Printability of hydrogels can be improved by increasing polymer concentration which helps to increase their stiffness. Therefore, in a dense polymer network, the cells can migrate and be mobile when provided with an aqueous environment. [Hospodiuk et al. 2017].

2.4. CLASSIFICATIONS OF HYDROGELS

2.4.1. Natural polymers

2.4.1.1. Gelatin

Gelatin is a natural polymer derived from the processing of animal proteins which is used in food and pharmaceutical industries [Gómez-Guillén et al., 2011; Liang et al., 2004]. Bones, skin, and connective tissues of animals are the extracting source of gelatin [Gómez-Guillén et al., 2002]. Gelatin have helical strands by self-association, leading to form a gel-like material at low temperatures. When the temperature increases, it reverts back to a random coil structure [Chiou et al., 2008]. Gelatin has less immunogenicity, promotes cell adhesion, differentiation, migration, and proliferation due to the Arg–Gly–Asp (RGD) groups retained from its precursor [Sakai et al., 2009].

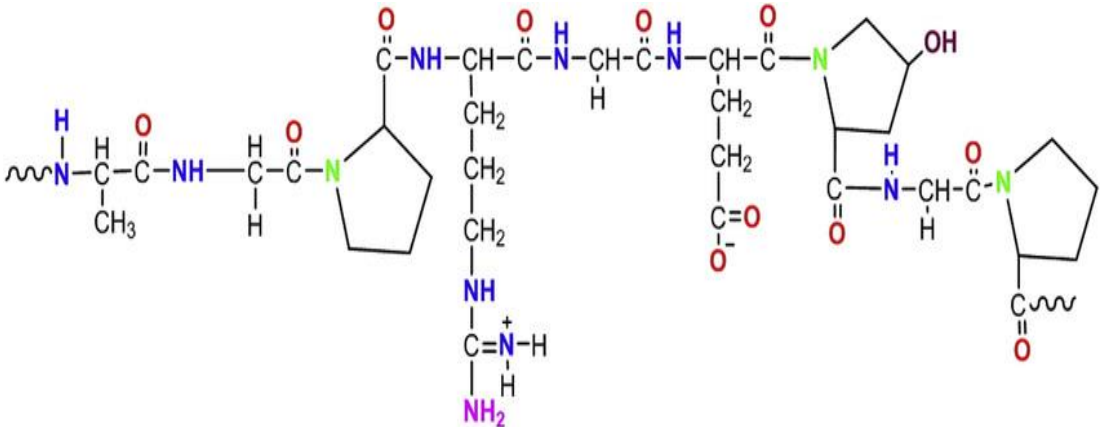

Figure 2. 3. Structure of gelatin [Thakur et al. 2017]

By thermally-induced crosslinking gelatin obtains its gel form and at 37°C it becomes liquid. The mass of unmodified gelatin gel decreases by 50% after about 10 hours of incubation and within 24 hours the gel completely dissolves [Sakai et al., 2009]. To avoid dissolution, a variety of chemical crosslinking systems have been examined; But, crosslinking agents are cytotoxic for the living cells loaded in the constructs so these methods are problematic *for in-situ and in-vivo* applications [Liang et al., 2004]. Transglutaminase, one of the popular enzymatic crosslinker, has been effectively used [Jin and Dijkstra, 2010]. Horseradish peroxidase (HRP) and hydrogen peroxide (H2O2) are the other new crosslinkers used [Sakai et al., 2009].In the *in vivo*, gelatin can be successfully gelled and stayed intact for one week without inducing necrosis in neighboring tissues [Sakai et al., 2009]. The cells exhibit long term viability when encapsulated into gelatin, but cell elongation is limited [Benton et al., 2009; Nichol et al., 2010]. Because of its poor mechanical properties the native form of gelatin is rarely used for bioprinting. Addition of glutaraldehyde, the chemical crosslinking agent, with gelatin makes them suitable for bioprinting [Hellio and Djabourov, 2006]. Gelatin polymer back bone has free amine groups which undergo nucleophilic addition reaction, simultaneously reacts with the two aldehyde groups of glutaraldehyde and carries out the dehydration reaction that produces an imine functional group usually mentioned to as a Schiff base [Hennink and van Nostrum, 2012]. Commonly, the pH of the medium determines the degree of gelation. Molecules which are capable of accepting or losing protons through a rise or reduction in pH are sensitive to a change in the local pH environment. Extrusion based bioprinting have been used for the

bioprinting of a hepatocyte-laden gelatin into a spatially-defined 3D structures. More than two months, hepatocytes stay viable and conducts their biological functions [Wang et al., 2006]. Droplet-based bioprinting of hydrogel such as gelatin is not commonly used. For liver tissue biofabrication, certain studies have been done by mixing fibrin with gelatin [Wei Xu et al., 2007]. Droplet-based bioprinting of gelatin/alginate blend has been presented by Boland et al. However, the top of the blended solution were printed by $CaCl_2$ solution [Boland et al., 2007]. Because of the viscoelastic properties, stability and capacity to hold the cells in exact positions without harming the cells, gelatin has been successfully used in laser-based bioprinting [Raof et al., 2011; Schiele et al., 2011].

2.4.1.2. Collagen

Collagen type I is a natural derived, biocompatible protein with a triple helical structure which is extensively used in bioprinting [Ferreira et al., 2012]. It is the main component of connective tissues and the most abundant protein in animals, occupies around 25% of the total protein mass. Collagen is an extremely conserved protein cross-species generating minimal immunological reaction. Due to the numerous integrin-binding domains in collagen matrix enables good cell adhesion, enhances cell attachment and cell growth. For bioprinting, collagen type I has been used, But it has some drawbacks such as, at lower temperatures it remains in liquid state and at higher temperature or neutral pH it forms a fibrous structure. The gelling of collagen takes about half an hour with a temperature of 37 °C. Three dimensional bioprinting of collagen construct was difficult because of the slow gelation time, since beyond 10 minutes the deposited collagen remains liquid. Similarly, the gravity pulls down the cells before the gelation taking place. As a result the cells are non-homogeneously distributed onto the collagen. Thus a supporting hydrogel is necessary for preventing the above stated problems as well as the low mechanical properties and instability of collagen. Collagen by itself as a bioink has been developed through an extrusion-based bioprinting [Smith et al., 2004]; still, it generates promising results when it is mixed with Pluronic® [Homenick et al., 2011]. Collagen is appropriate for cell growth because, after the 24 hours of post-bioprinting, the number of cells significantly improved. Perfusion of a completely cross-linked bioprinted construct can be done [V.

Lee et al., 2014]. Bioink material derived from collagen can also be produced by droplet based bioprinting method; although, collagen wants to be deposited before the onset of crosslinking [Deitch et al., 2008]. A bilayer skin graft was fabricated by Boland's group that generated a neo-skin on mice that mimic native skin with micro-vessels. Also they studied the cells with the help of collagen as a bioink material [Yanez et al., 2015]. Inkjet bioprinting of collagen was limited due to its fibrous micro-architecture, hence micro-valve bioprinting has been used. For skin burn management, valve-based bioprinter is used for developing a fibrin-collagen bioink using any one of the cell type like AFSCs or mesenchymal stem cells (MSCs) were fused into the wound spot [Skardal et al., 2012]. Laser-absorbing material was coated with a thin layer of collagen by using laser-based bioprinting; and a laser pulse can be used for transferring the sticky collagen easily [Michael et al., 2013; Hospodiuk et al. 2017].

2.4.2. Synthetic polymers

2.4.2.1. Pluronic

Pluronic is a synthetic polymer brand-named as Pluronic® F-127 and it is a poloxamer-based polymeric compound. It is a good surfactant due to the two hydrophilic blocks between a hydrophobic block in its polymer architecture [Mesa et al., 2005]. Depending on its molar mass, percentage of composites, functionality, and temperature of crosslinking Pluronic® is classified as 11 different types, and differ from 10 to 40°C accordingly [S. Wang et al., 2015].When increasing the temperature of Pluronic® the reverse gelation takes place and it starts to crosslink. Structural integrity of Pluronic® copolymer is very poor, that is, not exceed more than few hours and it is erode quickly; however, copolymer of Pluronic® with polyethylene glycol(PEG) derived hydrogels is used for controlled drug delivery applications [Gong et al., 2009]. Incorporation of methacrylated hyaluronic acid with Pluronic® increases its mechanical strength [Müller et al., 2015]. In a 3D Pluronic® background the bone marrow derived mesenchymal stem cells could be capable to intermingle with each other and after the four days culture, the adipogenic induction started [Vashi et al., 2008]. Cells are viable in pure Pluronic® up to five days and after that the cell viability was decreasing dramatically. Even there was a higher concentration of Pluronic® with

an addition of 60 nM hydrocortisone, the cell viability was well-kept [Khattak et al., 2005]. In bioprinting applications, UV light can be used for Pluronic® crosslinking, but the duration of exposure and type of radiation used were directly affect the cell viability [Johnson, 2011] and the metabolic activity of cells can be affected by the initiator concentration. Thermal degradation of gels can be prevented by chemical crosslinking [Masutani et al., 2014]. Enzymatic crosslinking of Pluronic® can be carried out by self-assembled micelle formation in the two ends of PEO side chains [Lee et al., 2011]. Mechanical strength of Pluronic® was increased with enzymatic crosslinking but the thermally reversible properties of Pluronic® do not change. Above 20°C, Pluronic® turn into highly viscous and it shows shear thinning behavior which was suitable for extrusion based bioprinting. However, depending on the concentration of Pluronic®, the transition from liquid to gel was determined by the heating system around the needle; and after deposition of the construct, temperature was controlled by a heating plate, both heating system and a heating plate should be required. In a homogeneous suspension, the semi-liquid state of Pluronic® is difficult to maintain with the aim of cell viability. A cooling system is required for a bioink reservoir to hold in a lower temperature, if the bioprinting takes a long process. To produce a complex construct, the reversible properties of Pluronic® can be beneficial. At room temperature or higher temperature Pluronic® appears in a solid form. Hence, to develop a perfusable channel within bulky cell-laden constructs, this solid form of Pluronic® is enclosed with a different kind of hydrogel, then it is liquefied by placing it in 4°C [Wu et al., 2011]. Droplet-based bioprinting is challenging for Pluronic® because of its higher viscosity and thermo sensitive nature. Pluronic® is non-viscoelastic, preserves a solid covering on the quartz support and cannot transfer thermal energy to kinetic energy, which is necessary for jet formation; hence it cannot be used for laser-based bioprinting. [Hospodiuk et al. 2017].

2.5. IDEAL BIOINK

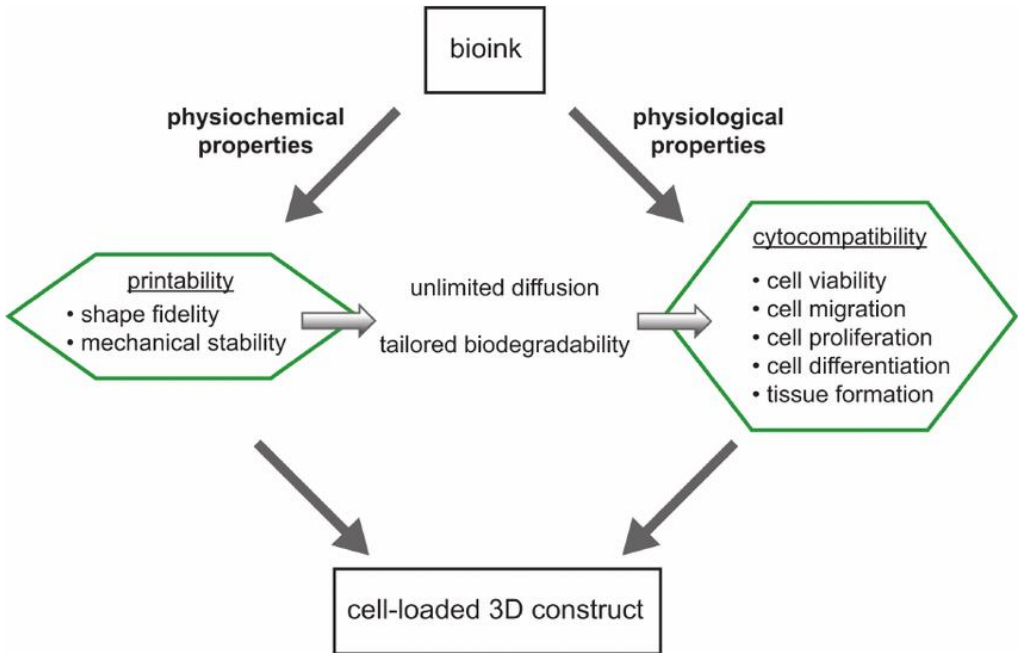

Figure 2. 4. Schematic representation of an ideal bioink [DeSimone et al. 2015].

2.5.1. Printability

For the tissue engineering applications, various hydrogels were developed by modifying the chemical backbones of polymers. The bioprintability of hydrogel was determined by various factors like, rheological properties and the target bioprinting modality. So all hydrogels cannot be bioprintable. Bioprinting processes were subdivided into three main classes based on their mechanisms. The main three techniques are extrusion-based bioprinting (EBB), laser-based bioprinting (LBB) and droplet-based bioprinting (DBB) [Dababneh and Ozbolat, 2014; Gudupati et al., 2016; Ozbolat and Hospodiuk, 2016]. According to each bioprinting technique, there are some requirements for bioink properties. Extrusion-based bioprinting is again derived into pneumatic and mechanical. In EBB, the hydrogels having a non-Newtonian fluid behavior, i.e., shear rate and viscosity are dependent on each other [Jungst et al., 2016]. EBB also suits a hydrogel with shear thinning and thixotropic behavior. The extruding of shear thinning hydrogel was easy, and its random polymer chain became aligned into a favorable direction, by a shear force applied on it.

The time dependent shear thinning behavior is also known as thixotropic behavior, due to this property, and the bioink undertakes a stable form at the barrel, and it has low viscosity inside the nozzle tip during extrusion, also at post-bioprinting the stability was regained. In extrusion based bioprinting, the supporting viscosity has been maintained from 30 mPa/s to 60×107 mPa/s [Mandrycky et al., 2016]. Depending on the hydrogel concentration, viscosity also varies. For example, Pluronic® F-127 (25%) has a viscosity of 30 mPa/s but the concentration increases to 40%, the viscosity of Pluronic® F-127 was >600×106 mPa/s [Chang et al., 2011]. When the cell density was under 2x106/mL, there was no significant difference in the viscosity of bioink [Ouyang et al., 2016]. To eliminate the attachment of bioink on the surface of the nozzle tip, it should have ideal surface tension properties and low adhesion which enables the formation of filaments than a droplet formation (due to the surface tension). The rapid gelation properties make the bioink from spreading, and retain its shape, so maintaining a fast gelation is necessary. The substrate used for bioprinting should have high surface roughness and low wettability, and it should be properly placed, which helps the bioink to retain its shape by sticking on the substrate.

Other bioink types involve additional processes and customized systems for the extrusion setup, however the hydrogel bioprinting is a comparatively direct process because the layer-by-layer fabrication system is incorporated with a crosslinking mechanism. For example, customized extrusion-head is needed for loading of cell aggregates. For delivering the tissue spheroids into the medium, a pipette unit is needed to load it [Tan et al., 2014]. Nozzle clogging is caused by the loading of cell aggregates into the pipette unit due to the aggregation of the tissue spheroids. In addition, poor tissue development may result because of the essential close contact between spheroids post-bioprinting is not accomplished. To promote the cell aggregation, an additional support structure (for example agarose mold) can be printed in tandem, makes cell pellet extrusion relatively simple. If there is no necessity for a molding structure or a delivery medium, solid form of tissue strands can be bioprinted. It is important that, a proper bioprinting is enabled when the strands are engineered with malleable and mechanically strong properties [Yu et al., 2016]. A 3D printing frame is mandatory for supporting the dECM in bioprinting until the complete gelation is over. Pati et al established the 3d printing of dECM with PCL in his recent work, where when printed construct of PCL

is used for *in vivo* implantation, and degradation of PCL structure is challenging [Pati et al., 2014]. Microcarriers can be directly bioprinted, but nozzle clogging problems occurs when they were loading at higher densities. [Hospodiuk et al. 2017].

2.5.2. Biocompatibility

Biocompatibility is defined as the ability of a material to be implanted *in vivo* without causing deleterious local or systemic reactions. [Hoffman AS. 1; 64:18-23, 2012]. Alginates are bioinert and it does not interact with cells, so the cell adhesion of alginate matrix was poor. It was due to the lack of cell adhesion moieties on the alginate back bone, which causes the apoptosis of cells via anoikis after encapsulation. Denaturated form of collagen known as gelatin, has cell adhesive RGD sequences, and are capable of reverse thermal gelation. So, adding gelatin to alginate will overcome its limitations [Chung et al. 2013]. Addition of gelatin will increase the cytocompatibility and viscosity of alginates, and the storage modulus also increases with the viscosity, when composite was cooled below the gelatin's gelation temperature, causing an improved fidelity in printing. [Chimene D, Lennox KK, Kaunas RR, Gaharwar AK. 1; 44(6):2090-102, 2016.]

Hydrogel type, hydrogel concentration, and the post encapsulation time are the factors affecting the cell viability. Recently few studies showed the cell viability of numerous hydrogels. The effect of cell viability of Matrigel, twenty five percentage Pluronic® F-127, two percentage alginate, and one percentage agarose were discussed in one study [Fedorovich et al., 2008]. The results show that there is no significant difference in cell viability after five hours of incubation; but after 24h, 20% of cell are viability visible in Pluronic®. Matrigel and alginate preserved their cell viability around 90% after the seven days, although this same period of time agarose decreased to 70% in their cell viability, but in case of Pluronic® there is no viable cells are detected after seven days. The cell viability and proliferation between the printed and manually deposited scaffolds are showing no significant variation in the same report. Bioprinting modality is another factor that impact on cell viability, whereas cells are viable more than 85% and 95 % after Droplet based bioprinting and Extrusion based bioprinting respectively [Chang et al., 2011]. Concentration of hydrogel also depends the cell survival, upto100% of viability is possible with a blend of 5% gelatin and 1% alginate

composition; but after 6hrs post bioprinting of 10% gelatin and 1% alginate, the viability of cells decreased to 70% [Ouyang et al., 2016]. About 90% viability is results from a 2% alginate concentration, although 35% viability results from a 6% concentration [Yu et al., 2013]. If the aggregate size is small, cell viability of cell-aggregate based bioink material is high; but when the aggregate diameter size increase to 400-500 μm, cell viability is decreasing dramatically [Ozbolat and Hospodiuk, 2016]. Over 95% of viability shown by the bioprinted dECM, which is the highest rate of viability among hydrogels has been reported in various articles [Jang et al., 2016; Pati et al., 2014, 2013; Hospodiuk et al. 2017].

2.5.3. Cross-linking condition

Crosslinking of polymer precursors can be undertaken before or after 3D printing to form a hydrogel. Cytocompatibility of crosslinking reactions can be carefully examined because, the encapsulation of cells are mostly carried out in this step for all cases. Mostly physical crosslinking reactions are used for sterilization and physical crosslinking method such as ionic, thermal and enzymatic (for example, thrombin with fibrinogen) are generally used crosslinking methods. Physical crosslinking reactions are mild reactions and they cannot intermingle with cells, reversible gelation can be experienced. But for *in vivo* studies this gentle reactivity leads to an unstable crosslinking and unbalanced in bulky media reservoirs. Although the interstitial tissue fluid or an extra-gel concentration is under the intra-gel concentration, calcium based crosslinker is seen seeping out from alginate in physical crosslinking. Plasma proteins and proteases may interrupt the hydrogen bonded crosslinking in gels to opposing *in vivo* environment. Chemical crosslinking is another method, but it cannot be used, if bio-orthogonality is required. Alternative crosslinking methods are UV crosslinking, Thiol Michael type addition reactions, and “click” reactions, all of these are successfully used for cell encapsulation. [Rutz et al. 2017].

In bioprinting, free radical photopolymerization is the most commonly used technique for chemical crosslinking of cellular hydrogels. This process takes place within three steps, such as initiation, propagation and termination. In the first step, initiation of free radical is formed by the irradiation of required dose of light energy, on to the photosensitive system having unsatured prepolymer, cells and initiator. In the

second step, the formation of crosslinking between polymer chains as well as new free radical generation happens due to the reactive species propagate through the vinyl moieties on prepolymer in solution. Then the chain growth mechanism ensues increasing the number of crosslinking in the system with a formation of highly crosslinked network. Even though, under biocompatible conditions, natural and synthetic hydrogels undergo rapid fabrication via free radical photopolymerization. But oxygen inhibition, lack of control over the crosslinking kinetics, and the generation of heterogeneities within the hydrogel network are the limitations of this crosslinking method. Random chain polymerization results an inhomogeneity's in the network, which considerably influence the mechanical integrity and swelling behavior of the constructs [Pereira et al. 2015]. The crosslinking reaction between thiol and alkene undergoes a thiol Michael type addition. An emerging reaction, for e.g., copper-free reaction between azides and activated alkynes is known as click reaction. Bioinks are commonly crosslinked by UV- crosslinking, whereas limited use of thiol Michael type was found and bioink also uses click reactions. Enzymatic crosslinkers that begins physical crosslinking, where genipin and transglutaminase are the enzymatic covalent cross-linkers which is used to manipulate hydrogel degradation and mechanical properties. Dynamic cross-linking or "adaptable linkages"— guest–host interaction, biorecognition, hydrophobic interactions, hydrogen bonding, ionic cross-linking, and dynamic covalent reactions are the set of subdivision of crosslinking reactions used for 3D printing. Material extrusion through a very thin nozzle and the ability to maintain extruded filament shape can be perfectly produced by this set of reactions due to its shear-thinning and self-healing properties. [Rutz et al. 2017].

There are three major issues associated with the photopolymerization reaction during the cell encapsulation. The harmful effect of UV irradiation is the leading problem of this reaction. Another problem is photo initiators dissociated into radicals are likely to be cytotoxic. Similarly, unreacted double bonds cause local inflammation. To reduce the side effect of these irradiations, UV light source or visible light source can be used for cell encapsulation applications. The cell damage caused by the UV irradiation can be eliminated, via choosing appropriate light wavelengths, intensity and irradiation time. There are various studies taking place to develop a photosensitive

system (hydrogel precursors and photoinitiators) that can undergo photo crosslinking reaction by the introduction of a safe visible light wavelength.

Photoinitiators have a major role alike light source in photopolymerization. The free radicals generated by the photoinitiators promotes the formation of crosslinking between polymer chains. Though, during the photopolymerization reaction, these radicals react with the cellular components which may induce the cytotoxicity and DNA damage through direct contact or the formation of reactive oxygen species [Pereira, 2015]. This is the major limitation of using photoinitiator.

Another alternative is to use redox initiators which have been used earlier with great success earlier for initiating polymerization. Normally persulphate/bisulphate combinations are used to initiate polymerization at room temperatures. This technique has been successfully tried before for hydrogels in the preparation of contact lenses etc.

2.5.3.1. Redox polymerization

Polymerization reactions utilizing redox initiators and producing free-radicals through oxidation reduction is known as redox polymerization. Redox initiation also called redox catalysis, or redox activation. The main advantages of redox initiators are their lower activation energy of the reaction, which result in a radical formation at wide range of temperatures, i.e., the initiation reaction occurs relatively at lower temperatures (0-50^{o} C). Redox initiation has been widely employed in free-radical polymerization.

The reaction between oxyacids of sulphur and persulfates form efficient redox systems. Sulfite, bisulfite, bisulfate, thiosulfate, metabisulfite and dithionate are the examples for oxyacids of sulphur. The initiation step involved in this method were represented as:

$$S_2O_8^{2-} + S_xO_y^{n-} \rightarrow SO_4^{\cdot -} + SO_4^{2-} + \dot{S}_xO_y^{(n-1)-}$$

$$SO_4^{\cdot -} + HOH \rightarrow H\dot{O} + HSO_4^{-}$$

Figure 2. 5. Reaction mechanism of persulfate/ metabisulfite

The free-radical anions, $\dot{S}_xO_y^{(n-1)-}$ and $SO_4^{\cdot -}$ initiates the polymerization reaction. Polymers without hydroxyl end groups were probably found in this type of redox pairing, because the reducing sulfoxy compounds or the resultant radicals derived from the reduction of sulfoxy compounds were good scavengers for OH radicals.

Polymerization of acrylamide, acrylonitrile, methacrylamide and methyl methacrylate can be done using persulphate with different reducing agents. [Sarac AS, 1999]

Hydrogels can be prepared by different ways. Redox initiators allow the polymerization or the hydrogel formation quickly at very low temperatures. The starting material was in the form of liquid, and it allows the casting of gels into various shape and forms. Also, the gels can retain their shapes without swelling or deswelling in water [Refojo et al. 1965].

2.5.4. Degradability

The type of hydrogels selected or the blend of that hydrogel, concentrations, temperature, *in vitro* or *in vivo* conditions and existence of external additives are the factors that depends on the degradability of bioink materials. Thermosensitive hydrogels are extremely sensitive to external circumstances and liquefy easily. Similarly when the environmental conditions varies, the original shape of the hydrogel was lost. Moreover, a hydrogel with a hydrolytic or enzymatic labile component, degradability can be varied [Nicodemus and Bryant, 2008]. Choice of different chemical formulations is limited due to the cells present in hydrogels, but still uphold the mechanical strength. Micro carriers slowly degrade than hydrogels, due to their hard polymer composition, hence it may release cytotoxic substances. Briefly, rate of degradation of 3D constructs must be planned according to the uses [Hospodiuk et al. 2017].

2.5.5. Sterilizability

Sterility is the challenging factor in the field of bioprinting research. There are many kind of sterilization methods for bioink polymers. Bioink polymer solutions can be sterilized by using filtration and autoclave, Polymer solids such as proteins are sterilized by gamma irradiation. These techniques have their own advantages and disadvantages. About 70% of ethanol can be used for sterilization of numerous materials, however it cannot be eliminate all kind of contaminations, so it is not an ultimate method used for clinical translations. Sterilization must be carried out for all kind of stuff, such as cartridges, nozzles and substrates, manipulators like forceps, spatulas and fluids that may come contact with bioinks. Additionally, sterilization

method such as Ethylene oxide, plasma irradiation, and 10% bleach can be used for sterilizing equipment's, but limited uses in case of bioinks. [Rutz et al. 2017].

2.6. GelMA AS BIOINK

Methacrylamide modified gelatin is known as gelatin methacrylamide. It is called Gelatin Methacrylate or Gelatin methacrylamide or GelMA. The main advantage of GelMA hydrogel was its 3D printability, and has the same properties like gelatin such as cell adhesion, biocompatible, biodegradable etc. Within two months the GelMA can be degraded *in vivo*. Thus, GelMA is widely considered for scaffold fabrication [Shi, W., He, R., & Liu, Y. et.al. 2015].

GelMA is a gelatin derivative material having a majority of methacrylamide groups and a minority of methacrylate groups. In the presence of a photocurable initiator under the exposure of a UV light, gelatin was subjected to radical polymerization to form a covalently crosslinked hydrogel. ECM consists of collagen, which is the main component of tissue, similarly, Gelatin encloses various arginine-glycine-aspartic acid (RGD) sequences, which helps the cell attachment along with the target sequences of matrix metalloproteinase (MMP) that are apt for remodeling of cell. Better solubility and less antigenicity are the advantages of gelatin than collagen. Also gelatin undergoes physical crosslinking at a low gelling temperature and covalent crosslinking of gelatin is possible by several chemical reactions. With the help of a photoinitiator or redox initiator, methacryloyl substituent groups to will undergo crosslinking with gelatin due to the polymerization of the methacryloyl substituents. At a mild condition such as room temperature, neutral pH, aqueous environment, this polymerization occurs so, there is a temporal and spatial control of the reaction. This can be used for the microfabrication of the hydrogels which can be used to produce distinctive patterns, 3D structures, and morphologies, also provides ultimate platforms to control the behavior of cells, to study cell-biomaterial interactions, and for tissues engineering. Less than 5% of the amino acid residues involve in the chemical modification of gelatin by methacrylic anhydride (MA) reaction, and the functional amino acid motifs such as the RGD motifs and MMP-degradable motifs will not be considerably influenced. The RGD motifs of GelMA do not have a reactive site to interact with MA, Hence it has good cell adhesive properties.

The *in vitro* enzymatic degradation study of GelMA hydrogels using type I and type II collagenases which is also called MMP-1 and MMP-8, correspondingly, continues at quicker rates, showing the presence of MMP-sensitive motifs in GelMA. Furthermore, several different applications such as tissue engineering, drug and gene delivery of GelMA hydrogels have been studied in terms of its physical and biochemical properties [Yue et al. 2015]. GelMA was used to print a 3D mesh-like scaffold by Dubruel et al. GelMA is extruded through a nozzle with a temperature controller in a cold jelly state, and the printed shape as well as entire 3D structure was retained by the cold gel for a short time. When printing is completed, Curing of printed object can be done by a UV light source. In printing process, GelMA was pre-seeded with cells and extruded. Throughout the printing and culturing of cells, a sufficient biocompatible microenvironment was provided by GelMA, and it simplifies printing process. The lack of vessel network is the main issue in tissue engineering for transporting the nutrition and wastes. GelMA is used for functional human vascular networks in a considerately designed 3D printing method by Ali group. Initially, a vessel like structure was printed using agarose in an extrusion based printer. Agarose hydrogel was acting as a sacrificial template and in cold environment it possesses jelly state. Then GelMA solution with SMC cells is transferred into the agarose filled container. The hollow vessels are formed by removing the agarose template by water flushing after the UV light curing of GelMA takes place. An infusible live blood vessel model is formed by seeding the endothelial cells on to the hollow vessel surface. This hollow channels formation drastically enhances the cell viability. Hence, vascularized constructs and hydrogel can be developed by this method [Shi et al. 2015].

Gelatin modified to GelMA by altering its ε-amino group with methacrylic anhydride or methacrylamide (MA) will improve its mechanical properties. While redox polymerization is more effective method than other technique such as photopolymerization, thermal application, UV ray s, and ϒ-irradiation. GelMA copolymerized with hydroxypropyl methacrylate (HPMA) may result an increase in its mechanical properties [Resmi, R et al. 2017].

2.7. LIMITATIONS OF GelMA BIOINK

In tissue engineering, tissues require extensive load-bearing properties, and GelMA hydrogels used for TE have some limitations such as poor mechanical properties and short degradation time [Han et.al.2017, Wang H et.al. 2014]. Hydrogel network crosslinking density was a factor which affects the mechanical properties and degradation of hydrogels [Bryant SJ, Anseth KS., 2002]. As the crosslinking density increases, compressive modulus also increases. And through the modification of crosslinking density of hydrogel, the concentration of precursor macromer can be controlled [Metters AT et.al. 2000]. Also the hydrogel matrix concentration could not influence to alter the macromer concentration. Gelatin contains RGD sequences, therefore crosslinking density was important for gelatin based hydrogels. According to the variations in the gelatin concentration, the crosslinking densities of RGD also vary. Similarly, the prolonged crosslinking time increases the crosslinking density. But the cell viability decreases by the long UV-irradiation time [Li et al. 2017]. The challenge in 3D printing of GelMA hydrogel is the balancing of physical printability and biological functionality of tissue engineered scaffolds application [Yin et al. 2018].

2.8. GAP AREA

Briefly, one of the main applications of 3D bioprinting is the development of tissue engineered scaffolds. Hence, maintaining the stability of scaffolds is important. The literature discussed above shows that, there are various limitations in the field of 3D bioprinting. The properties of bioinks determine the quality of 3D bioprinted constructs. Concentration, mechanical strength, gelation time, and viscosity are the crucial factors associated with the bioinks. Increase in the concentration of hydrogels enhances the strength of the gel which will affect the cell viability. Similarly, when the concentration of hydrogel decreases, the viscosity also decreases significantly, which affects the printability [Yin et al. 2018] Therefore, balancing of physical printability and biological functionality of the 3D bioprinted construct is essential. Also, from the literature it is known that, UV induced crosslinking is reported to causes cell damage [Pereira, 2015]. Therefore, alternate initiators which do not damage the cells and are also inexpensive may be the need of the hour [Resmi R et al. 2017].

2.9. HYPOTHESIS

Virgin gelatin methacrylamide gels have limitations in use as potential bioink due to their weak mechanical properties and high swelling characteristics. In this work we hypothesize the incorporation of hydroxyl propyl methacrylate in limited amounts into gelatin methacrylamide to induce optimum properties for potential use in bioprinting. The use of redox initiators also provides an alternative to UV based photoinitiation which is conventionally used in 3D bioprinting making it more cost effective.

2.10. OBJECTIVES

- To synthesis GelMA and characterize its physiochemical properties
- To develop a GelMA-HPMA based bioink using redox initiators and characterize its physiochemical properties
- To test the cytotoxic effect of GelMA-HPMA based bioink
- To check the possibility of cell encapsulation in GelMA-HPMA based bioink
- To test the printability of hydrogel

CHAPTER 3

MATERIALS AND METHODS

3.1. DEVELOPMENT OF GelMA-HPMA BASED HYDROGEL

3.1.1. Materials used

Gelatin Type A (From porcine skin), and Methacrylic anhydride (94% pure) were purchased from Sigma-Aldrich Chemical Company Inc., USA. Hydroxypropylmethacrylate (HPMA, 97% pure) was procured from Merck, Germany. Potassium persulphate (LR, 98% pure), Potassium Metabisulphite (95% pure) was purchased from NICE, India, and Loba Chemie, India, respectively.

3.1.2. Synthesis of Gelatin Methacrylamide (GelMA)

About 10g of Type A gelatin (derived from porcine skin) was weighed and dissolved in 100ml phosphate buffer saline (PBS) at 50˚C and stirred until it dissolved completely. Methacrylic anhydride (0.5 ml) was added drop by drop to the above solution and continuously stirred at 200 rpm for 3hrs. After 3 hours, the original solution was diluted 5 times by adding warm PBS (40˚C) solution to stop the reaction. To remove the salts and unreacted methacrylic acid, dialysis of the resultant solution was carried out using a 12-14kDa cutoff dialysis tube in deionized water at 40˚C for 1 week. The obtained viscous solution was then kept in a deep freezer at -80ºC and lyophilized in a lyophilizer (Christ Alpha 1-4 LD, Germany) when an off-white GelMA crystallized after the lyophilization (Figure 3.2). It was stored at -80 ˚C in a deep freezer for further use. The reaction between Gelatin and Methacrylic anhydride was shown in Figure 3.1.

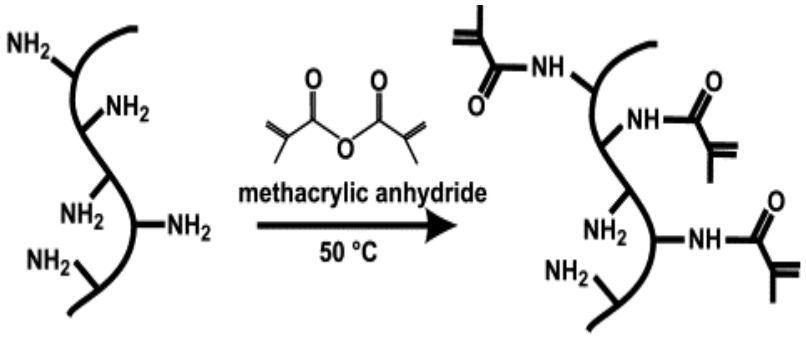

Figure 3. 1. Structure of GelMA formed by the reaction between gelatin and methacrylic anhydride [Nichol, J. W, 2010].

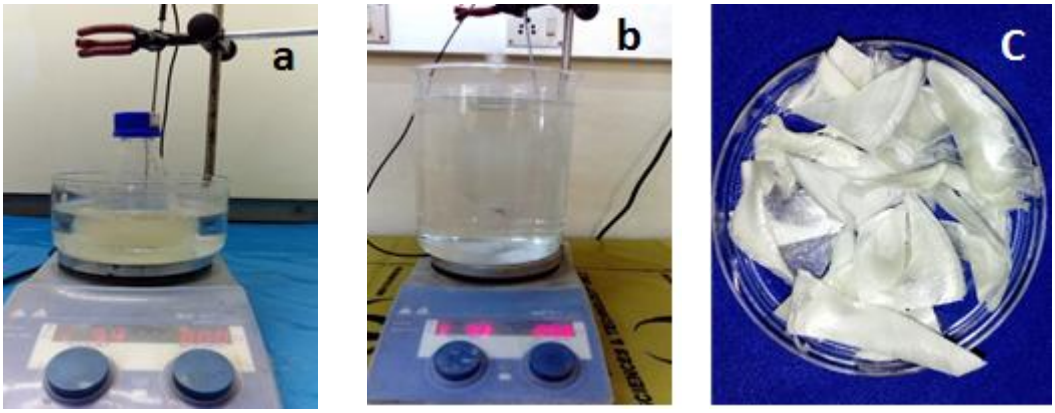

Figure 3. 2. Photograph showing the step by step Synthesis and Dialysis of GelMA

3.1.3. Refractive Index of Hydroxypropylmethacrylate monomer

The chemical structure of HPMA can be represented as

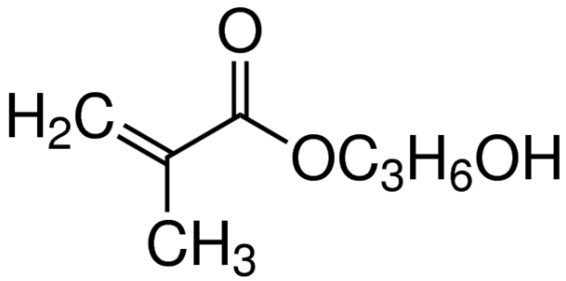

Figure 3. 3. Structure of Hydroxypropylmethacrylate

HPMA was distilled before use under vacuum for removing the stabilser. The purity of distilled HPMA was determined by measuring the refractive index using a refractometer (3T, ATAGO, JAPAN). Initially the surface of the prism and the test piece were cleaned. A monomer droplet was placed onto the main prism center and the upper lid was closed. Upon illumination and viewing through the eyepiece, the color compensator knob was rotated to get the boundary line between the upper red and lower blue regions. The boundary line was then aligned with the intersection of the crosswire in the refraction field of vision and scale reading was noted as the refractive index of the sample at room temperature.

3.1.4. Preparation of redox initiator system

Persulphate redox initiators such as Potassium persulphate and potassium metabisulphite were used for this method. 3% solution by weight was prepared by dissolving 3g initiator in 100ml distilled water. Both this solutions were prepared separately and kept at room temperature for further reactions. The reaction mechanisms involved in this peroxide redox initiators are shown below.

Redox initiated polymerization reaction allows much better biocompatibility than UV- cross linked mechanism. Mostly, potassium persulfate ($K_2S_2O_8$) and potassium metabisulfite ($K_2S_2O_5$) were used as a redox system. In this reaction, radicals were generated when they react each other (Figure 3.4).

$$S_2O_8^{2-} + S_2O_5^{2-} \rightarrow SO^{4-*} + SO_4^{2-} + S_2O_5^{-*}$$

$$SO_4^{-*} + H_2O \rightarrow HSO_4^{-} + OH^*$$

Figure 3. 4 . Reaction mechanism of persulphate/matabisulphite redox system

The reaction involves three steps, initiation, propagation, and termination. In the first step, the SO_4^{-*} and $S_2O_5^{-*}$ radicals attached with the monomer molecules. Then the propagation step occurs and the chain grows respectively. In the termination step, it happens either by termination by coupling (recombination of two growing chains) or

by disproportionation (a growing chain can subtract a radical from another growing chain) and forming a double bond.

3.1.5. Preparation of the GelMA-HPMA hydrogel matrix

GelMA was warmed with distilled water with constant stirring and heated to 40˚C and HPMA was added in drops to the mixture so as to prepare a 20% solution. Various formulations by varying the GelMA-HPMA ratios were prepared as shown in Table 2.1. Subsequently redox initiators (3%) were mixed with this solution and the total solution should be maintained in a ratio of 5: 0.5:0.5 having monomers, initiator 1, and initiator 2 respectively. Redox initiators such as Potassium persulfate and Potassium metabisulphite were used for this reaction. On mixing the initiators the hydrogels are formed according to its varying gelation times at room temperature.

Table 3. 1. Different concentrations of monomers

Sample Code	Wt. %	
	GelMA	HPMA
G100HP0	100	0
G95HP05	95	05
G90HP10	90	10
G80HP20	80	20
G60HP40	60	40

3.2. CHARACTERIZATION OF HYDROGEL SYSTEMS

3.2.1. Structural characterization

Fourier Transform infrared spectroscopy (JASCO 4200 Series FTIR Spectrometer, USA) was used for the characterization of Gelatin and GelMA by using KBr pellet method although GelMA-HPMA based hydrogels were characterized by using Attenuated total reflection (ATR) method.

In KBr pellet method, about 0.1 mg of gelatin or GelMA was weighed and ground with KBr in a ratio of 1:300 in a smooth agate mortar. A thin transparent disc was made from the resultant fine powder, by applying a pressure about 150 kg/cm^2 for 3minutes using a hydraulic hand press. KBr alone was used as the control.

After warming the instrument, the background measurement of control was quantified (bare KBr pellet). CO_2 and moisture peak was effectively eliminated after this recording. Next, the sample disc was observed using FTIR. The resultant spectra was obtained between 4000-400 cm^{-1} ranges, by 40 scans at 4 cm^{-1} resolution. And using the software, baseline corrections, smoothening, and labeling of peaks of FTIR spectra were processed.

In Attenuated total reflection method, the samples of 6 cm length and 1cm width with 1mm thickness was placed onto the zinc selenide (ZnSe) horizontal flat plate sample holder ATR assembly of a FTIR spectrometer. Background measurements were done without the sample. The spectra were measured between 4000-400cm^{-1} ranges with 40 scans per sample at a resolution of 4 cm^{-1}.

3.2.2. Nuclear Magnetic Resonance (NMR) spectroscopic analysis of GelMA

Proton nuclear magnetic resonance (^{1}H NMR) spectroscopy was used to assess the chemical modification of gelatin. About 10 mg mL^{-1} of methacrylated gelatin was dissolved in D_2O at a temperature of 50 °C. ^{1}H NMR spectra were recorded with a Bruker AMX 500 spectrometer.

3.2.3. Opacity test

The opacity of G100HP0, G95HP05, G90HP10, G80HP20 and G60HP40 hydrogels were measured by using an ADA approved black and white opacity display chart according to the ADA specification No 27. The opacity shall be represented in contrast ratio $C_{0.70.}$ Contrast ratio is the ratio of the luminance of the brightest color (white) to that of the darkest color (black) that the system is capable of producing.

About 1mm thick samples were prepared in a Teflon mold, after gelation, it was immersed for 24hr in distilled water at 37±1˚C.The hydrogel sheets were placed on the surface of black and white display chart and compared the opacities of specimen with the three opal glass standard (Delrin) having $C_{0.70}$ values of 0.35, 0.55 and 0.95 respectively. A film of distilled water shall cover the specimen and the standards. Also, observed the space between them and the black and white background during the test.

The opacity of the samples either equal to or between the opacities of standard, which was visually observed.

3.2.4. Optimization of Gelation time

About 2ml of different hydrogel solutions (G100HP0, G95HP05, G90HP10, G80HP20 and G60HP40) were prepared by mixing the monomers with the redox initiators in a test tube and polymerization with time was monitored by tilting the test tube horizontally till it stops flowing at a temperature of 22 ˚C. This gelling time was noted. Mean and standard deviation was calculated. Optimized the gelling time of each gel at 22 ˚C.

3.2.5. Swelling analysis

The swelling studies of G100HP0, G95HP05, G90HP10 and G80HP20 hydrogel systems were carried out. Three samples of each different composition was prepared in a 24 well plate and after gelation, it is removed from the well and the initial weight (Wi) of the gel was noted. Subsequently, samples were immersed in distilled water for 24hrs at 37 ºC. After 24hrs, the distilled water was wiped out carefully from the surface of the swollen hydrogels samples and weighed subsequently (Ws). The percentage swelling was calculated using the equation:

$$\%\, Swelling = \frac{Ws - Wi}{Wi} \times 100$$

3.2.6. Mechanical testing

The compressive modulus of G100HP0, G95HP05, G90HP10 and G80HP20 hydrogels were determined using universal testing machine (UTM, Instron 3365, UK). The cylindrical samples were cast in a 48 well plate and the hydrogels having approximately 7mm diameter and 10mm height were prepared. The compressive modulus of the samples was measured by applying the load till the sample compressed to the half of its original height. A 100N load cell was used for the test with the crosshead speed at a rate of 10 mm /min. Mean and standard deviation of modulus was calculated using the following equation.

$$\text{Compressive modulus } (MPa) = \frac{\text{Compressive Load}}{\text{Compressive Extension}}$$

3.2.7. Micro-computed tomography analysis

The porosity and microstructure analysis of lyophilized hydrogels samples were conducted using micro-computed tomography (MicroCT 40, Scanco, Switzerland). A PMMA tube was used as a sample holder and the samples were placed on the sample holder for X-ray attenuation. The scanning was done with a high X-ray energy (45kV) and an intensity of 177μA having 10μm resolution (2D slice thickness). The cone beam algorithm was used to prepare the 2D reconstructions. The 3D image was also collected from the machine by setting appropriate threshold values.

3.2.8. Rheology of Bioink

Rheological property of G90HP10 solution was evaluated by a rheometer (MCR102, Anton Paar, USA) equipped with a Peltier element for temperature control. A cone-plate geometry (CP25) with a diameter of 24 mm and a cone angle of 2.009˚ was used in this measurements. At first, the sample was placed on the plate at 26.35°C (RT) to completely fill the gap size (0.105 mm) between two plates. The measurements of viscosity were performed by varying the time from 0 to 200s with a rotational motion at 26°C, and the shear rate was maintained at 100 s^{-1}.

3.3. *IN VITRO* EVALUATION GelMA-HPMA HYDROGEL

3.3.1. Commercial reagents

Dulbecco's Modified Eagle's (DMEM: F12) medium, foetal bovine serum (FBS), antibiotic-antimycotic (AbAm), trypsin-EDTA (Gibco BRL, USA), MTT (3-(4, 5-Dimethylthiazol-2-yl)-2, 5-Diphenyltetrazolium Bromide) (Sigma Aldrich, USA), 4',6-diamidino-2-phenylindole (DAPI) (Sigma Aldrich, USA), Ethidium bromide and Calcein AM (Invitrogen, USA) were obtained from the respective sources mentioned in brackets.

3.3.2. Cell seeding

Samples of 0.7 cm diameter discs with 2mm thickness sterilized by ethanol sterilization were used for the *in vitro* evaluation of the GelMA-HPMA hydrogel. L929 fibroblast cell line was used for the *in vitro* studies. Cells were cultured under standard cell culture conditions with media change. Cells at a seeding density of 5000 cells/ cm^2 were used for the study.

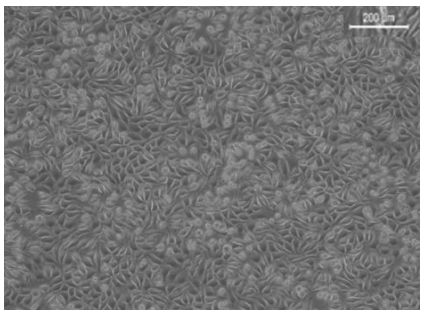

Figure 3. 5. Phase contrast image of the confluent fibroblast L929 cell line

3.3.3. Direct contact assay

Cytotoxicity test was evaluated using direct contact method. The hydrogel G90HP10 was used for cell culture analysis. The sterilized samples were placed on to the top of the confluent layer of fibroblast cells to evaluate cytotoxicity. The cells seeded on cell culture plate (TCPS) were taken as control. The cells were incubated with the samples at 37 ± 2 ºC with 95% relative humidity and 5% CO_2 in CO_2 incubator up to 72 ± 2 h and cells was examined under phase contrast optical microscope for morphological changes in cells as well as cellular response around the test samples.

3.3.4. MTT assay

The cell viability evaluation of the hydrogel G90HP10 was done after 72 h of incubation using 3-(4, 5-Dimethylthiazol-2-yl)-2, 5-diphenyltetrazolium bromide or MTT assay. MTT assay is a colorimetric indicator of cell number or viability by means of mitochondrial dehydrogenase activity. After specific time period, the cells were gently washed with PBS and 1.0 ml of MTT solution (1 mg/mL) was added per well and incubated for 2 h at 37 °C, 5% CO_2 in a humidified atmosphere. During this time, mitochondrial dehydrogenase activity will reduce MTT into an insoluble purple-colored formazan product which can be solubilized using dimethyl sulfoxide (DMSO).

After the incubation, the MTT reagent was removed and the insoluble formazan crystals were dissolved in 250 µL of DMSO with slight shaking. The absorbance was measured using microplate reader at 590 nm. The cells grown in TCPS was taken as control and compared with G90HP10 gel.

3.3.5. Two Dimensional Cell growth

For analyzing two dimensional cell growth, L929 fibroblast cells were seeded onto the top of the G90HP10 hydrogel discs placed on 35mm culture plates to evaluate cell attachment on the hydrogel and incubated for 24 h at 37 °C, 5% CO_2 in a humidified atmosphere. After 24 h incubation, the hydrogels were taken out and placed onto a new sterile culture plate and incubated at standard culture condition for 48 h. The plates were then visualized through phase contrast microscope to observe morphology of attached cells. For confirming fibroblast attachment and growth on the G90HP10 hydrogel, the hydrogel was stained for DAPI after 48 hour. Briefly, the hydrogel seeded with cells were washed with PBS after removing media, fixed with 3.7% formaldehyde, permeated by 0.2% triton x 100, washed and stained with DAPI for 3 minutes. Stained cells were washed with PBS and then viewed under fluorescence microscope (Leica, DMIRB, Germany).

3.3.6. Cell encapsulation of the hydrogel

To evaluate the feasibility of bioprinting of the G90HP10 hydrogel, cell encapsulation study was carried out. Initially, all the monomers used for the fabrication of the gels to be encapsulated with cell were sterilized using different standardized methods. GelMA was dissolved in PBS and was sterilized using pasteurization technique (70^{o}C for 15 minutes). The HPMA monomer and redox initiators were sterilized using sterile filtration (0.22 µm) and stored at 4^{o}C until use. The L929 fibroblasts were used for the encapsulation study. The gel was prepared as described before with cells. Cells at a density of 5,000 cells /100 µL of the total volume of gel was added into the gel before applying into the 96 well plate. A total volume of 0.05 mL was delivered into each well. The gel formation was visible within 1-2 min and the gels were allowed to stabilize for about 5 min and fibroblast basal medium was added.

GelMA along with the redox initiator without HPMA (G100HP0) and cell alone on the TCPS were taken as control.

3.3.7. Live/Dead staining of the cell encapsulated hydrogel

Fluorescence based live/dead assay was used to evaluate the viability of the cells encapsulated inside the hydrogel after 24 hrs. Live / dead staining was performed with calcein AM and ethidium homodimer-1 respectively. Live cells are distinguished by the presence of ubiquitous intracellular esterase activity, determined by the enzymatic conversion of the virtually non-fluorescent cell-permeant calcein AM to the intensely fluorescent calcein. The polyanionic dye calcein is well retained within live cells, producing an intense uniform green fluorescence in live cells (ex/em ~495 nm/~515 nm). EthD-1 enters cells with damaged membranes and undergoes a 40-fold enhancement of fluorescence upon binding to nucleic acids, thereby producing a bright red fluorescence in dead cells (ex/em ~495 nm/~635 nm). The assay was performed according to the manufacture's instruction after 24 hrs of incubation at standard culture conditions. The fluorescent imaging was done using confocal laser scanning microscope (Olympus Flouview FV3000).

3.4. PRINTABILITY TEST

3.4.1. Hand Printing

Initial printability trials showed the G90HP10 hydrogel to possess viscosity nearly optimum for the printability in a bioprinter. Initially, 2ml syringe was fixed with a needle of 20 gauge size and about 2 ml of viscous hydrogel solution mixed with the redox initiators was taken in the syringe. The solution was injected manually at a constant speed before curing commenced. A line and different shapes were drawn manually on the glass slide to check the printability and curing characteristics. Chemical curing of the bioink was completed in 3 min. Its stability was checked after 30 minutes.

3.4.2. 3D printing feasibility using the developed bioink

A cube with 10 mm x 10 mm x 3.5 mm dimensions was designed in computer aided design software (Free CAD). The design was saved in stereolithographic

(*.STL) file format and imported into a 3D printer slicing application (Cura, open source) to generate the GCODE. The GCODE file was opened in the replicator 3D printer interface software to control a customized 3D Bioprinter (Alfatek Systems Inc. Kolkata, India).

A 5 ml syringe was filled with GelMA-HPMA solution containing the redox initiators (1%, 1.5% and 3%) loaded on the 3D bioprinter and the hydrogel (cube shape) was printed in a 60 mm non-cell-adherent culture dish at 22 °C. A tapered nozzle with 1500 mm orifice was fixed and a print speed of 3.5 mm/s and a layer height of 6 mm were maintained.

CHAPTER 4

RESULTS AND DISCUSSION

4.1 CHARACTERIZATION OF RAW MATERIALS

4.1.1 Structural characterization of Gelatin and Hydroxy propyl methacrylate (HPMA) using FTIR spectroscopy

Gelatin and HPMA were characterized using FTIR spectroscopy. Gelatin shows a broad peak at 3294 cm^{-1} in the spectrum which corresponds to N-H stretching. A C-H stretching peak can be observed at 2933 cm^{-1}. Absorption peaks representing amide band I at 1659 cm^{-1}, amide II at 1548 cm^{-1}, amide III band at 1240 cm^{-1} and C-H deformation at 1444 cm^{-1} were also observed in the spectrum (Figure 4.1).

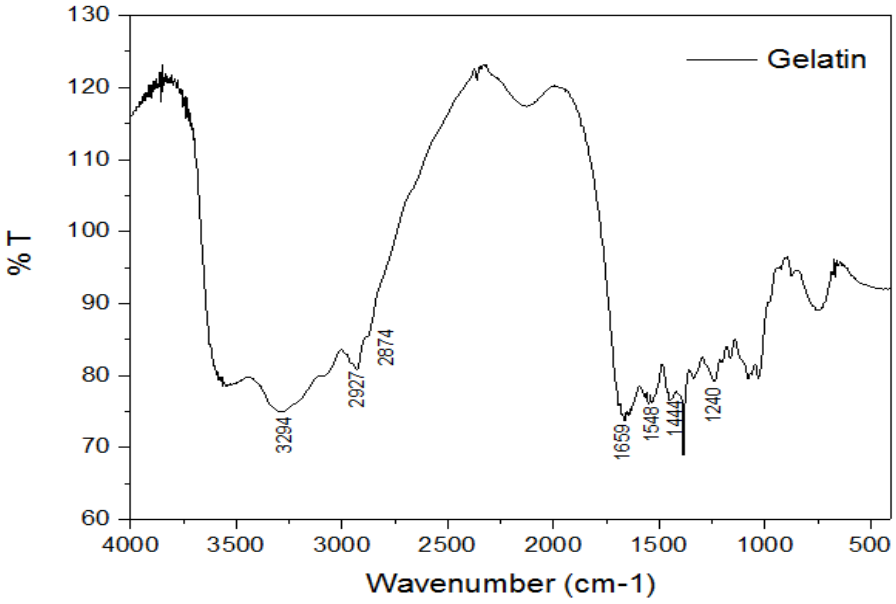

Figure 4. 1. FTIR spectra of Gelatin

FTIR spectroscopy revealed the characteristic peaks of hydroxypropyl methacrylate (HPMA). In the FTIR spectrum of HPMA, the strong hydroxyl (O-H) stretching was observed at 3421 cm^{-1}. C-H stretching peak at 2979 cm^{-1} , 2932 cm^{-1} and at 2887 cm^{-1}. An ester peak at 1710 cm^{-1} and an unsaturated C=C stretching can be observed at 1636 cm^{-1}.

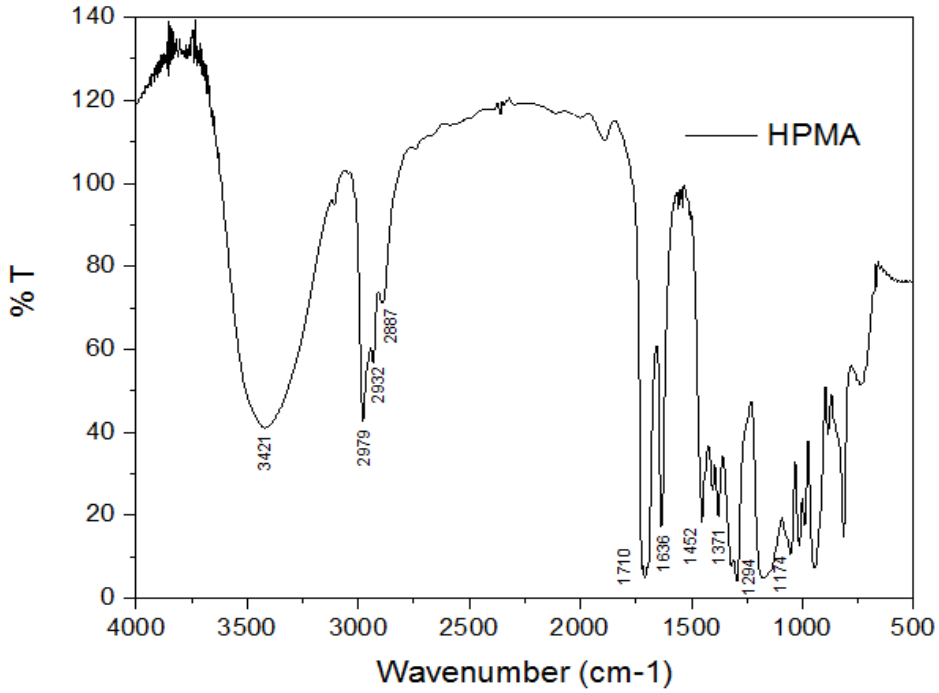

Figure 4. 2. FTIR spectra of HPMA

4.1.2 Refractive index of hydroxy propyl methacrylate

The refractive index of HPMA monomer was measured using a refractometer. The measured refractive index at 24 ^{o}C of HPMA was 1.443. It was found to be very close to the actual reference value of HPMA (1.447 at 20 ^{o}C). The distilled HPMA monomer has excellent purity.

4.2 PREPARATION OF GelMA

GelMA after the reaction of gelatin with methacrylic anhydride was obtained as off white flakes. Dialysis for a week made sure that all the residual monomers and unreacted components were washed out. Nearly 80-90 % yield was obtained during

synthesis. GelMA was stored in a deep freezer at -80 ºC in order to prevent moisture absorption. They were taken out, thawed to RT and used during preparation of GelMA-HPMA hydrogels.

4.3 CHARACTERIZATION OF GelMA

4.3.1 FTIR spectroscopy

GelMA showed the following specific vibrations: common O-H and N-H stretching peaks at 3392 cm^{-1}, at 3077 cm^{-1} respectively, saturated C-H stretching frequency at 2942 cm^{-1} and 2879 cm^{-1}. Amide I band at 1680 cm^{-1} and amide II band at 1530 cm^{-1}. A C=C unsaturated stretching peaks can be observed at 1635-1643 cm^{-1}.

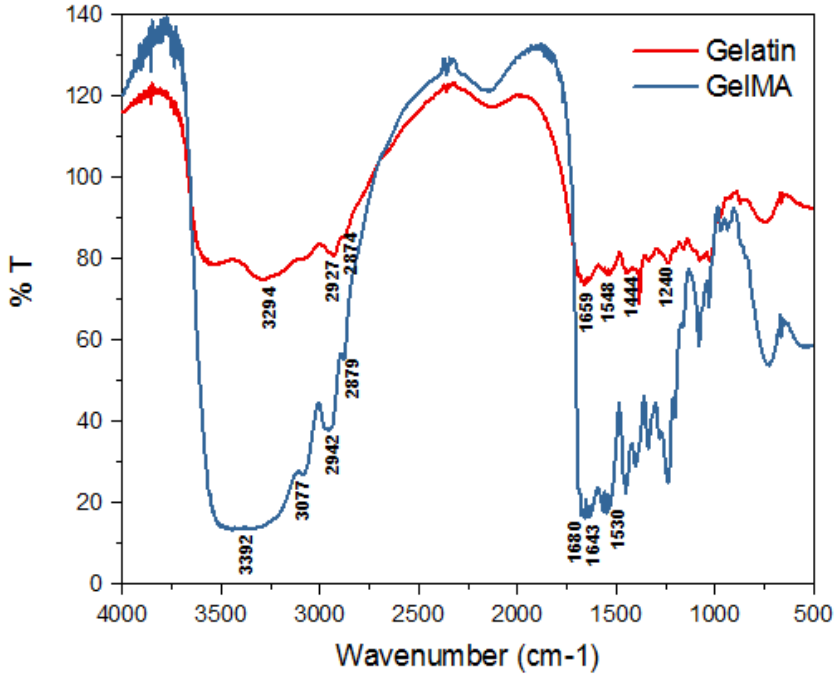

Figure 4. 3. FTIR spectra of Gelatin and GelMA

4.3.2 NMR spectroscopy

NMR spectra of GelMA shows two protons at 5.3 ppm and 5.5 ppm corresponding to the vinyl groups of methacrylic anhydride. New signals between 5.2 and 5.5 ppm in the spectra of Gelatin-MA indicates the conversion of additional functional groups in the gelatin molecules, therefore, it is confirmed that MA has been

successfully bound to the gelatin molecules. The above values are in consonance with reported values for GelMA [Amonpattaratkit P et al. 2017].

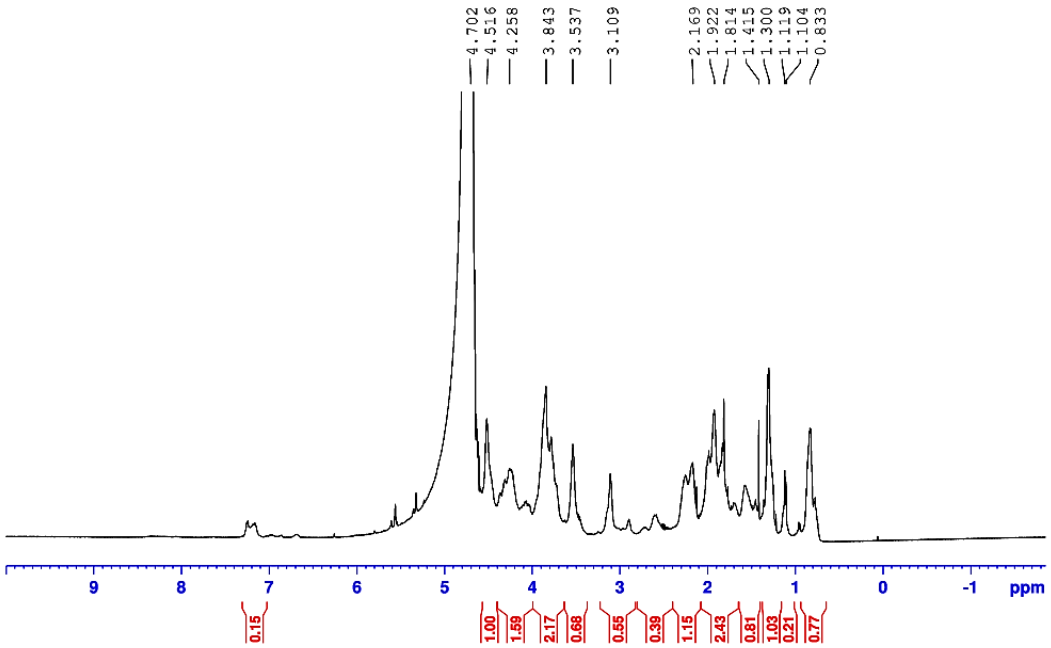

Figure 4. 4. NMR spectra of GelMA

4.4 PREPARATION OF GelMA-HPMA HYDROGEL

The redox polymerization of GelMA with HPMA was carried out in the presence of redox initiators. Redox polymerization takes place in three steps, initiation, propagation and termination. In the first step initiation of free radical formation occurs. $K_2S_2O_8$ and $K_2S_2O_5$ react with each other and form a radical anion $SO_4^{-\cdot}$. This radical anion reacted with the unsaturated carbon atom in the HPMA and form radical site. It further reacts with the unsaturated methacrylic branch of GelMA which is further propagated. Termination of this reaction may occur either by recombination or by disproportionation especially because of the resultant high molecular weight molecules. Earlier reports had suggested a 3% concentration of persulphate/metabisulfite combination to be optimum for use [Resmi R et al 2017]. The ratio of 5: 0.5:0.5 by volume was maintained for preparing hydrogel. It was observed that the polymerization was complete within three minutes. The resultant polymer was highly transparent as shown below:

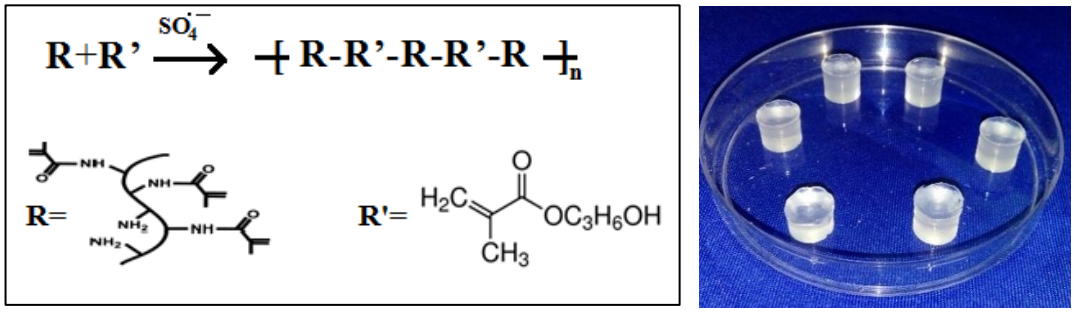

Figure 4. 5. Shows the reaction mechanism of GelMA-HPMA hydrogels and the resultant hydrogel respectively.

4.5 CHARACTERIZATION OF THE HYDROGEL SYSTEMS

4.5.1 Structural characterization of hydrogels using FTIR spectroscopy

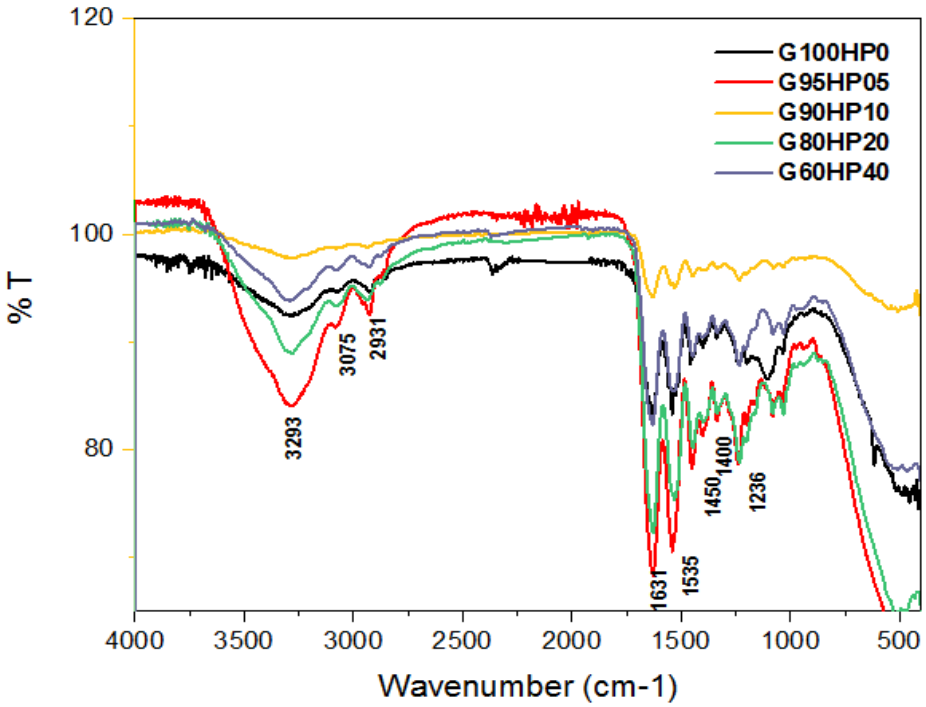

Figure 4. 6. FTIR spectra of hydrogels

The N-H stretching frequency can be observed at 3293 $cm^{-1}$and C-H stretching at 3075 cm^{-1} and 2931 cm^{-1}. The unsaturated peaks at 1635-1643 cm^{-1} have been replaced by the –C=O stretching secondary amide peaks at 1631cm^{-1}. Peak at 1535 cm^{-1} corresponds to amide bending. The disappearance of 1643cm^{-1} confirms the formation of binding between GelMA and HPMA.

4.5.2 Opacity

The results of opacity measurements are given in table 4.1. Out of the five samples tested, only G60HP40 showed a translucent character as shown in Figure 4.7. Rest of the samples had contrast ratios below 0.35 which indicated high transparent character.However when stored in water, all the samples tend to become highly transparent. Only G60HP40 hydrogel composition showed an opacity which is equal to the contrast ratio of 0.35. Translucency is an important property of required bioink as it helps in the easy imaging.

Table 4. 1. Contrast ratio of hydrogels

SI.No.	HYDROGELS	CONTRAST RATIO ($C_{0.70}$)
1	G100HP0	< 0.35
2	G95HP05	< 0.35
3	G90HP10	< 0.35
4	G80HP20	< 0.35
5	G60HP40	0.35

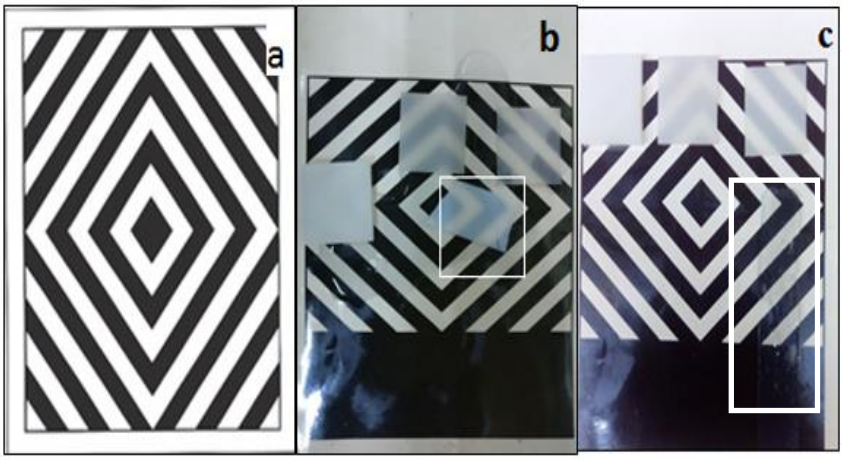

Figure 4. 7. Photograph showing (a) the black and white display chart (http://en.nbchao.com/p/753/) and (b) opacity testing of sample G60HP40 hydrogel (c) opacity testing of sample G90HP10 hydrogel.

4.5.3 Gelation time of hydrogels

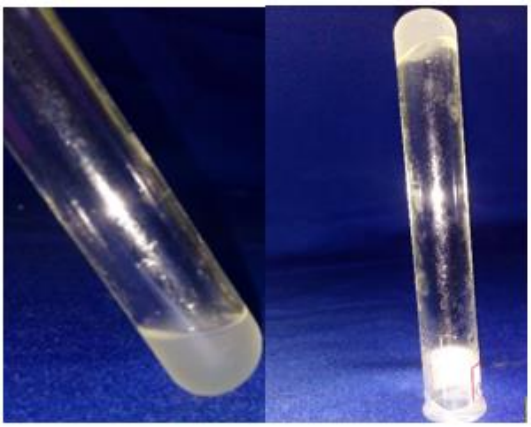

Figure 4. 8. Gelling images of G90HP10 hydrogel composition

The time for gelation of various hydrogel compositions are given in figure 4.9. It is clear from the figure that gelation time increases with the increasing amount of HPMA. This further supports the fact that, the radicals created from the redox initiators attacks the double bonds on GelMA and aids crosslinking when HPMA is added. This process of crosslinking is hampered causing a delay in the gelling of the hydrogels. It can be observed that when HPMA content goes up, the time of gelation also increases. There is a sharp rise in gelation time when HPMA concentration goes up from 20 % to 40 % in the mixture. A reason for choosing the G90HP10 formulation was because of the optimum gelation time obtained which is nearly 3-4 min.

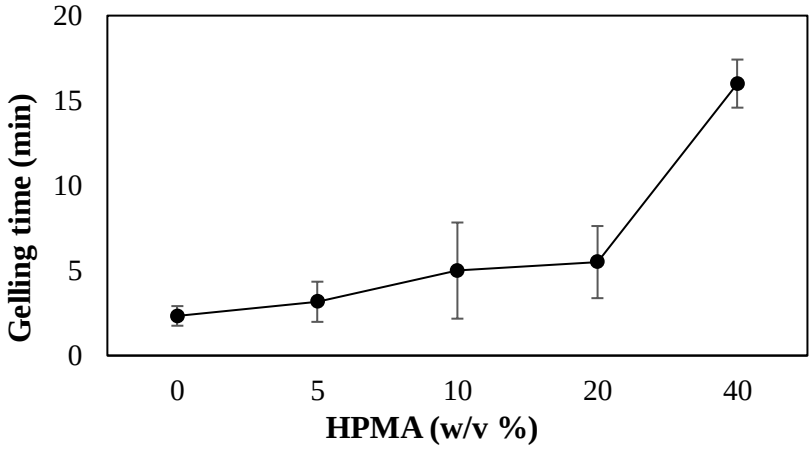

Figure 4. 9. Gelation time vs. HPMA (w/V %) graph

4.5.4 Swelling studies

Figure 4.10 shows the effect of HPMA concentration on swelling of the GelMA-HPMA hydrogels. Both G100HP0 and G95HP5 show a swelling of nearly 100-120%. However, when HPMA content rises to 10 parts as in G90H10, the swelling content decreases to nearly 68% which does not change significantly for G80HP20 also. The water intake of the samples tend to decrease when HPMA content increases which may count for the decreasing trend. For printing purposes, high water content like that in gelatin may be deleterious and an optimum content of 10 parts of HPMA will provide adequate flow properties through the printer. Hence choice of G90HP10 sample was found to be adequate for further printing studies.

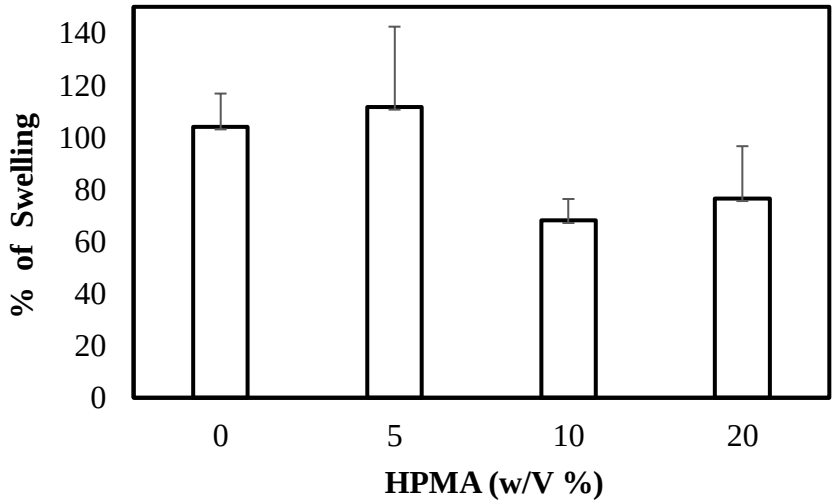

Figure 4. 10. Diagram showing the percentage of swelling of hydrogels

4.5.5 Studies on mechanical properties

Dependence of compressive modulus of GelMA -HPMA hydrogels are shown in figure 4.11. Compressive modulus tend to show an increase with increase in HPMA content. This may be due to increasing crosslinking that can happen with more HPMA in the hydrogel. Contribution of secondary forces such as van der waals forces and hydrogen bonding and intermolecular interpenetration will also contribute significantly for the increase in modulus values.

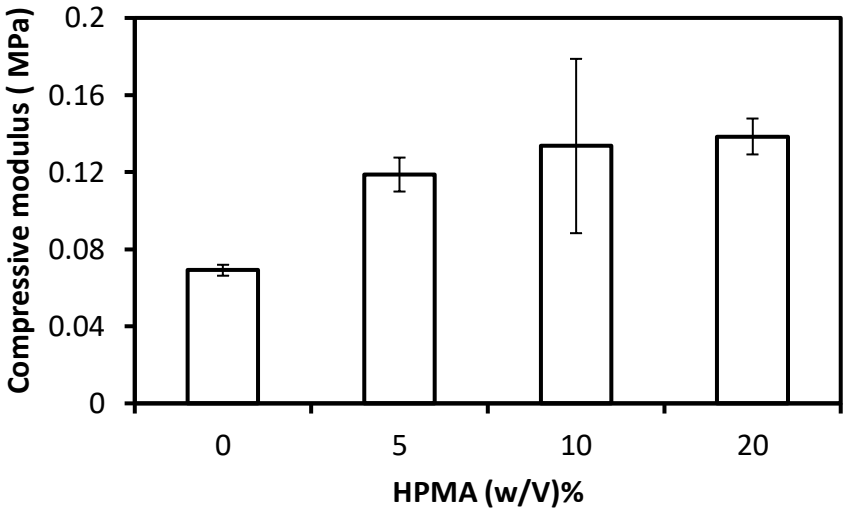

Figure 4. 11. Figure shows the compressive modulus of hydrogels

4.5.6 Micro computed tomography

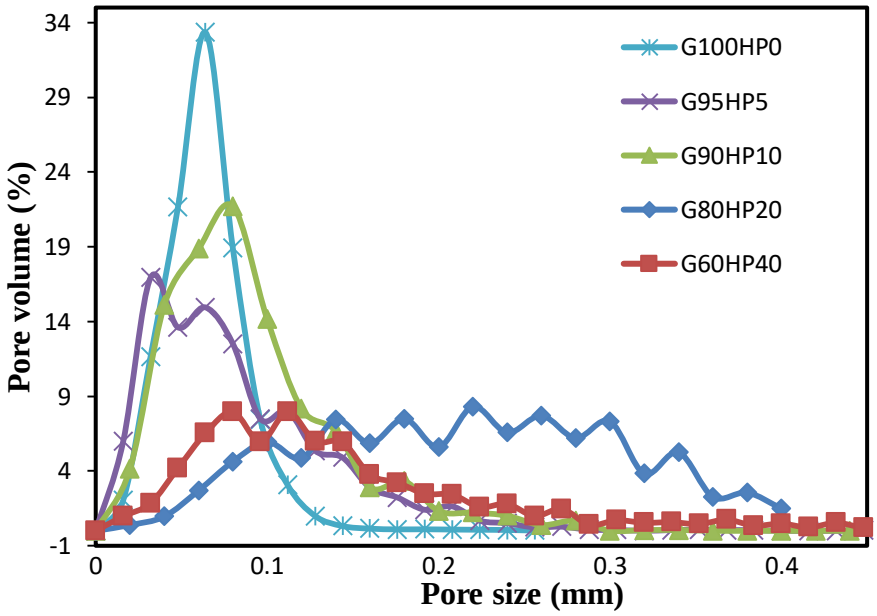

Figure 4. 12. Pore size distribution curves with volume for hydrogels studied.

Micro CT images depicting pore size distribution data, 3D images and porosity images reveal (Figures 4.12, 4.13 & 4.14) that pore size of the hydrogels in all cases to lie between 0 to 400 microns. All the samples were subjected to micro CT evaluation in the lyophilized dry state. However the maximum pore size tends to vary between 0-200 microns. As the HPMA content increases a larger pore size with broader

distribution seems to emerge as shown in the figure. GelMA alone shows a more narrow distribution of porosity (G100HP0). For G90HP10, the hydrogel of our choice for further studies, maximum pores had size less than 100 microns.

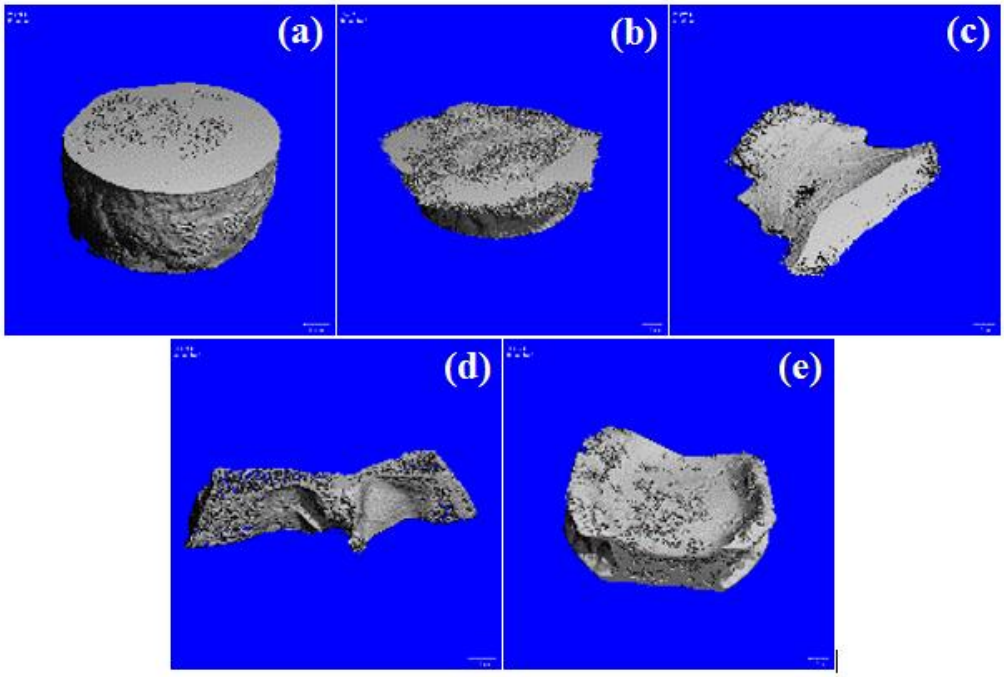

Figure 4. 13. Micro-CT 3D morphology images of hydrogels (a) G100HP0, (b) G95HP05, (c) G90HP10, (d) G80HP20 and (e) G60HP40 respectively.

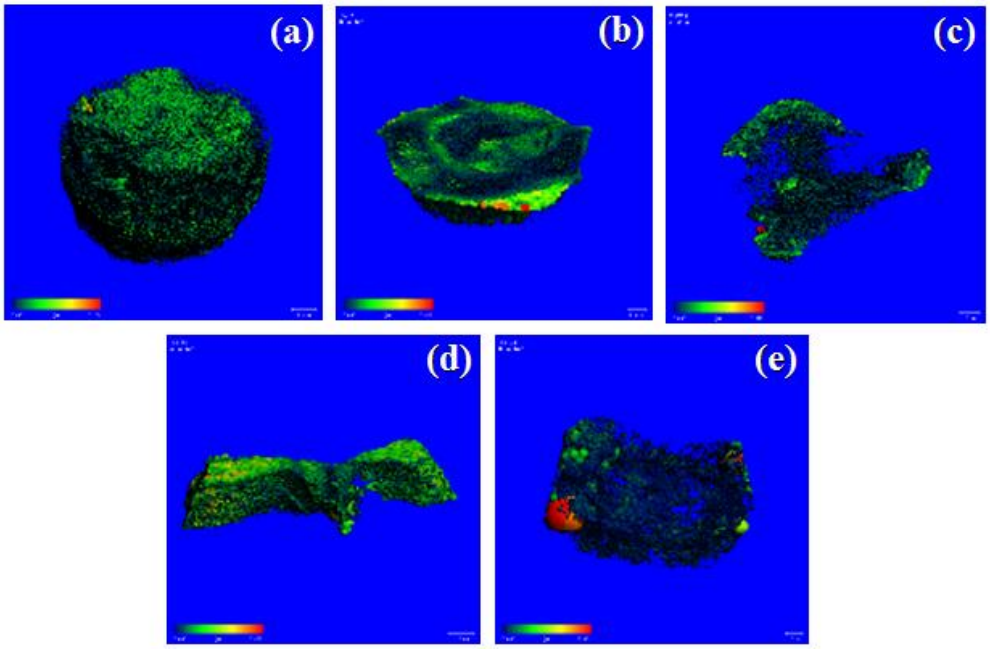

Figure 4. 14. Micro-CT porosity images of hydrogels (a) G100HP0, (b) G95HP05, (c) G90HP10, (d) G80HP20, (e) G60HP40 respectively.

4.5.7 Rheology

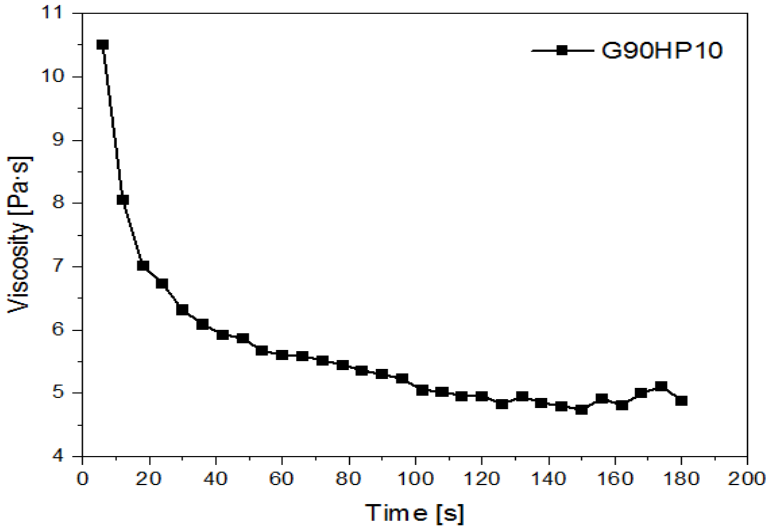

Figure 4. 15. Viscosity and time graph of GelMA90 and HPMA10

The objective of the determination of the viscosity value of the gel is important for printing purposes especially to study the flow characteristics. Rheological studies conducted in a rheometer show a shear thinning property with the viscosity values of the GelMA90-HPMA10 uncured hydrogel subjected to constant shear rate (100/s) to undergo a steady decrease in viscosity with increase in time as shown in Figure 4.15. This is typical of a viscoelastic solution that shows thixotropic properties. This experiment proves that GelMA-HPMA can be a candidate material as a bioink.

4.6 *IN-VITRO* STUDIES

4.6.1 Direct contact assay

Cytotoxicity test of the G90HP10 hydrogel was evaluated using direct contact method. The G90HP10 hydrogel incubated was viewed under phase contrast microscopy to observe the morphological and cellular response of the L929 fibroblast cells around the disc. There was no reduction in size of the hydrogel after sterilization, washing and culture for three days**.** Due to the high transparency of the material, cells that grow below the hydrogel could be easily viewed (Figure 4.16). Direct contact assay demonstrated that G90HP10 hydrogel did not induce any toxic effects and hydrogel were found to be cyto-compatible.

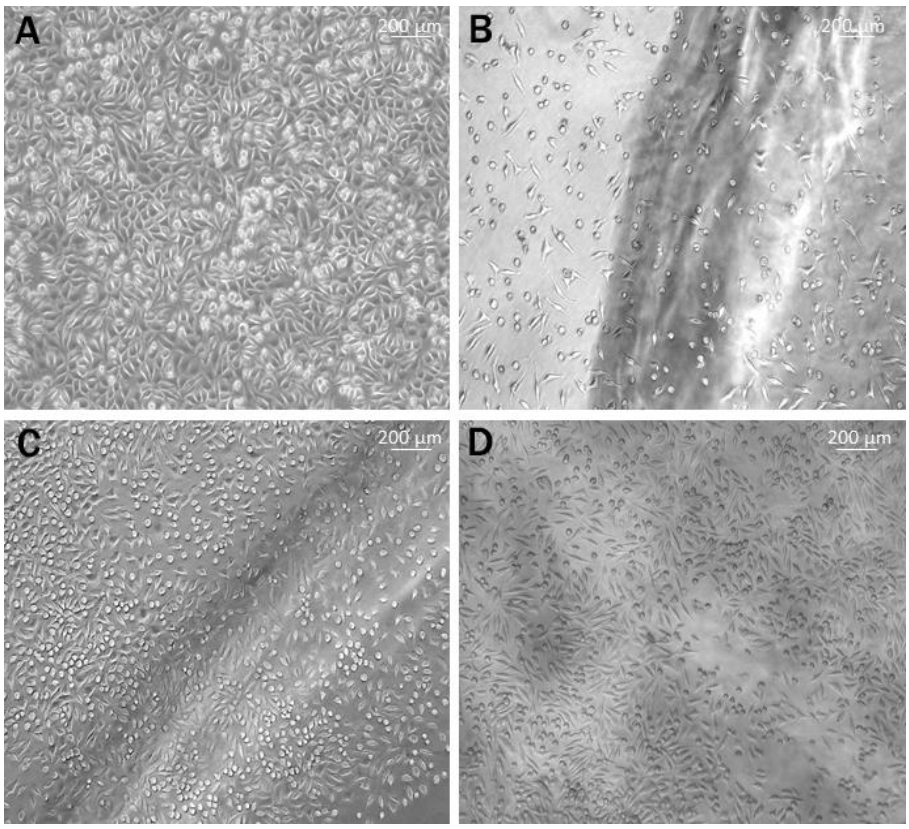

Figure 4. 16. Direct contact assay: A) Control cells grown on TCPS, B) Cells in contact with hydrogel after 24 h, C) Cells in contact with hydrogel after 72 h and D) Cells growing underneath the hydrogel.

4.6.2 Cell viability using MTT assay

The cell viability evaluation of the G90HP10 hydrogel was done after 72 h of incubation using 3-(4,5-Dimethylthiazol-2-yl)-2,5-diphenyltetrazolium bromide or MTT assay. The test showed significant difference in cell viability when compared to control cells grown in tissue culture polystyrene cell plate (TCPS) (Figure 4.17). This data conclusively indicates that the hydrogel is non-cytotoxic and promotes cell growth.

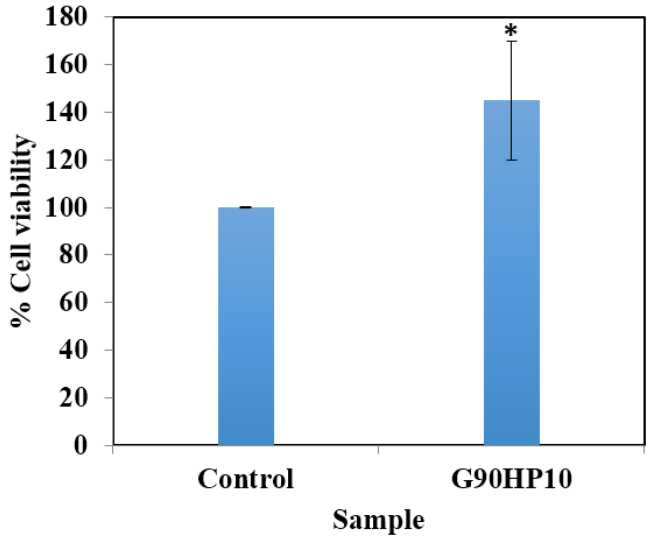

Figure 4. 17. Shows the percentage cell viability of control and G90HP10

4.6.3 Two Dimensional Cell Attachment

To evaluate the two dimensional cell attachment of G90H10 hydrogel, L929 fibroblasts cells were seeded on to the hydrogels. The phase contrast image shows the cells growing on hydrogel which was further confirmed by the DAPI staining. The DAPI staining of the hydrogel establishes the cell attachment on the hydrogel. The cells were migrating from the hydrogel to the surrounding. This confirms the cell attachment potential of the hydrogel.

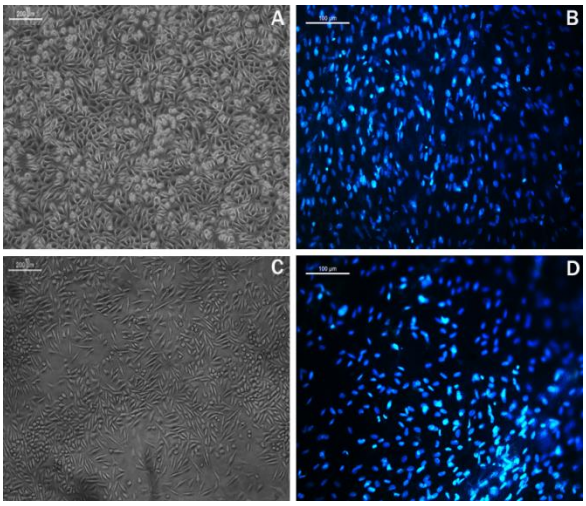

Figure 4. 18. Phase contrast image and fluorescent image of DAPI stained A& B) control L929 fibroblast cells on TCPS and C& D) L929 fibroblast cells on the G90HP10 hydrogel respectively.

4.6.4 Live/Dead Staining of the cells encapsulated in G90HP10 and G100HP0 hydrogel

The viability of cells encapsulated inside the hydrogel was evaluated using live/dead staining after 24 h. The cells were found to be viable inside the hydrogel. The live cells (green) inside the G90HP10 (Figure 4.19 C&D) were comparable with live cells inside G100HP0 (Figure 4.19 E&F). Dead cells (red) were very less in both the hydrogels. This suggests that the HPMA concentration does not induce any cytotoxicity. This confirms the cell encapsulation capacity of the G90HP10 hydrogel.

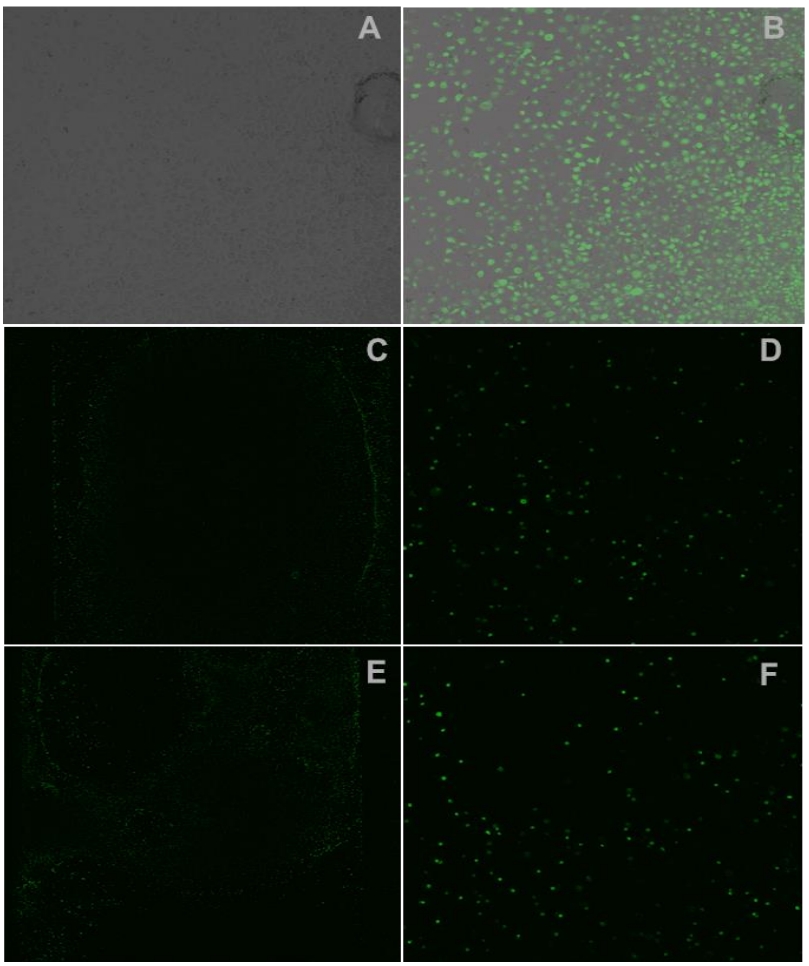

Figure 4. 19. Confocal images depicting Live/Dead staining of A) Phase contrast image of Control cells on TCPS, B) Control cells on TCPS, C & D) Cells encapsulated in G90HP10 and E & F) Cells encapsulated in G100HP0 hydrogel at different magnification.

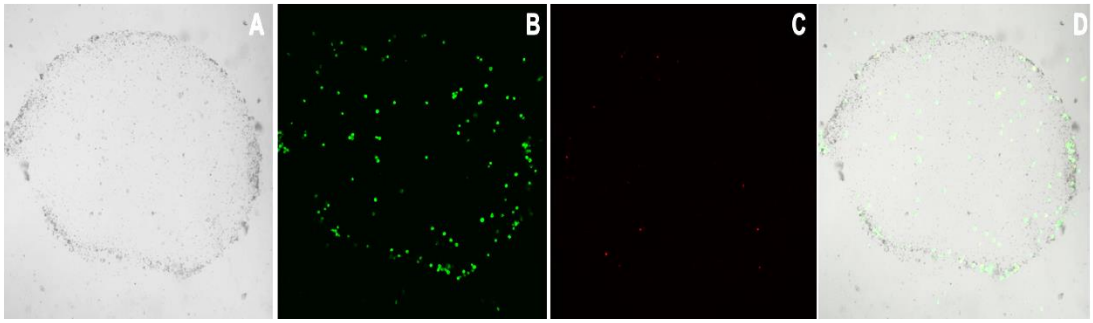

Figure 4. 20. Live /Dead staining of G90HP10 hydrogel : A) Phase contrast image of the hydrogel, B) Calcien AM staining for live cells inside the hydrogel, C) EtBr staining for dead cells inside the hydrogel and D) Merged image showing the hydrogel with live and dead cells (Magnification: 1.25 X)

4.7 PRINTABILITY

4.7.1 Printability

Initially hand printing was done manually in a 2 ml syringe which showed good flow properties for the gel (Figure 4.21).

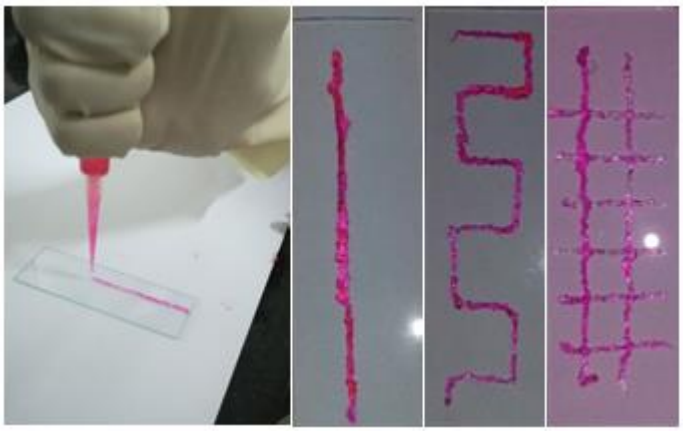

Figure 4. 21. Photograph showing the hand printing images of hydrogel G90HP10.

However printing was attempted with a 3D printer, a fast tendency to cure was observed within 3 min was observed when the concentration of initiator was kept at 3% which led to processing problems. Hence redox initiator concentration had to be optimized. So concentrations were reduced to 1.5% and 1% and gelation times were enhanced. Around 5 min gelation time was observed for 1.5% and 7-8 min for 1% redox initiator concentration.

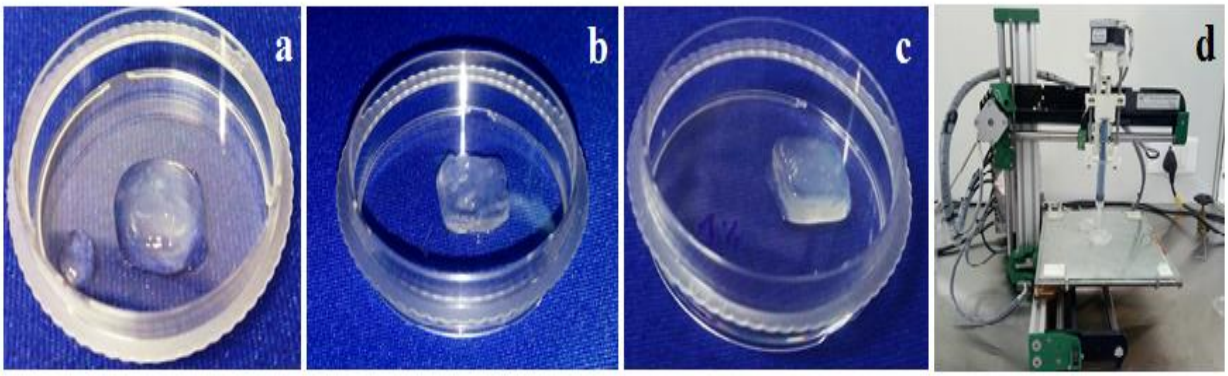

Figure 4. 22. Figure shows the 3D printing image of G90HP10 hydrogel (a) 3% redox initiator concentration (b) 1.5% redox initiator , (c) 1 % redox initiator and (d) 3D printer respectively

It was observed that better and easier printability was becoming possible than when the initiator concentrations were reduced to 1.5% and 1% gradually. Further printing studies could optimize the redox initiator having 1% concentration to provide good printability with no processing problems as can be observed from figure 4.22. It was observed however that the G90HP10 hydrogel could easily be used for printing purposes and has potential for use a bioink.

CHAPTER 5

SUMMARY, CONCLUSIONS AND FUTURE OUTLOOK

5.1 SUMMARY

Gelatin (Type A) was reacted with methacrylic anhydride to obtain gelatin methacrylamide (GelMA) which was characterized using spectroscopic techniques. The resultant GelMA was reacted with distilled hydroxypropyl methacrylate (HPMA) in various proportions to obtain hydrogel materials. The reaction was carried out at room temperature using redox initiators (persulphate/metabisulphite) combination. The hydrogel formation was observed within 3-4 min time. The hydrogels were characterized using spectroscopy and properties such as water swelling percentage, gelation time, mechanical properties, rheological characteristics, micro CT evaluation for porosity and opacity were evaluated. Out of the 5 systems studied, G90HP10 was optimized for further studies based on the results obtained. *In vitro* cytotoxicity studies using L-929 fibroblast cells, MTT assay and cell encapsulation studies were also conducted for the selected hydrogel. The gel so developed was tested for printability in a 3D bioprinter for potential use as a bioink. The concentration of the initiators was optimized to suit ideal flow properties for printing.

5.2 CONCLUSIONS

GelMA could be successfully synthesized in the laboratory by reacting gelatin with methacrylic anhydride and characterized using FT-IR and NMR spectroscopy. A hydrogel could be obtained by reacting GelMA with distilled HPMA by using redox initiators. Five different hydrogel systems were prepared and characterized and optimized for use as bioink. Out of the five systems studied, G90HP10 was found to have adequate swelling and mechanical properties and opacity to be selected for further biological studies. Cytotoxicity studies revealed the nontoxic character of the hydrogel and showed excellent cell viability. Cell encapsulation revealed that cells are viable inside the hydrogel. The hydrogel showed good printability properties by controlling the polymerization reaction by varying redox initiator concentration. The developed hydrogel has potential application as a bioink in 3D bioprinting.

5.3 FUTURE OUTLOOK

As evidenced by cytotoxicity and cell encapsulation studies, chances of bioprinting of the hydrogel incorporated with cells is possible. This particular character of the hydrogel along with the encapsulated cells needs to be studied further. If successful, this will be a novel hydrogel which can be used a bioink in future.

REFERENCES

Ahmed EM. Hydrogel: Preparation, characterization, and applications: A review. Journal of advanced research. 2015 Mar 1; 6(2):105-21.

Alge DL, Azagarsamy MA, Donohue DF, Anseth KS. Synthetically tractable click hydrogels for three-dimensional cell culture formed using tetrazine–norbornene chemistry. Biomacromolecules. 2013 Mar 8; 14(4):949-53.

Amonpattaratkit P, Khunmanee S, Kim DH, Park H. Synthesis and Characterization of Gelatin-Based Crosslinkers for the Fabrication of Superabsorbent Hydrogels. Materials. 2017 Jul 19; 10(7):826

Benton JA, DeForest CA, Vivekanandan V, Anseth KS. Photocrosslinking of gelatin macromers to synthesize porous hydrogels that promote valvular interstitial cell function. Tissue Engineering Part A. 2009 May 25; 15(11):3221-30.

Boland T, Tao X, Damon BJ, Manley B, Kesari P, Jalota S, Bhaduri S. Drop-on-demand printing of cells and materials for designer tissue constructs. Materials Science and Engineering: C. 2007 Apr 1; 27(3):372-6.

Bryant SJ, Anseth KS. Hydrogel properties influence ECM production by chondrocytes photoencapsulated in poly (ethylene glycol) hydrogels. Journal of Biomedical Materials Research Part A. 2002 Jan 1; 59(1):63-72.

Chimene D, Lennox KK, Kaunas RR, Gaharwar AK. Advanced bioinks for 3D printing: a materials science perspective. Annals of biomedical engineering. 2016 Jun 1; 44(6):2090-102.

Chiou BS, Avena-Bustillos RJ, Bechtel PJ, Jafri H, Narayan R, Imam SH, Glenn GM, Orts WJ. Cold water fish gelatin films: Effects of cross-linking on thermal, mechanical, barrier, and biodegradation properties. European Polymer Journal. 2008 Nov 1; 44(11):3748-53.

Chung JH, Naficy S, Yue Z, Kapsa R, Quigley A, Moulton SE, Wallace GG. Bio-ink properties and printability for extrusion printing living cells. Biomaterials Science. 2013; 1(7):763-73.

Deitch S, Kunkle C, Cui X, Boland T, Dean D. Collagen matrix alignment using inkjet printer technology. MRS Online Proceedings Library Archive. 2008 Jan; 1094.

DeSimone E, Schacht K, Jungst T, Groll J, Scheibel T. Biofabrication of 3D constructs: Fabrication technologies and spider silk proteins as bioinks. Pure and Applied Chemistry. 2015 Aug 1; 87(8):737-49.

Drury JL, Mooney DJ. Hydrogels for tissue engineering: scaffold design variables and applications. Biomaterials. 2003 Nov 1; 24(24):4337-51.

Ferreira AM, Gentile P, Chiono V, Ciardelli G. Collagen for bone tissue regeneration. Acta biomaterialia. 2012 Sep 1; 8(9):3191-200.

Furth ME, Atala A, Van Dyke ME. Smart biomaterials design for tissue engineering and regenerative medicine. Biomaterials. 2007 Dec 1; 28(34):5068-73.

Gasperini L, Mano JF, Reis RL. Natural polymers for the microencapsulation of cells. Journal of the Royal Society Interface. 2014 Nov 6; 11(100):20140817.

Gómez-Guillén MC, Giménez B, López-Caballero MA, Montero MP. Functional and bioactive properties of collagen and gelatin from alternative sources: A review. Food hydrocolloids. 2011 Dec 1; 25(8):1813-27.

Gong CY, Shi S, Dong PW, Zheng XL, Fu SZ, Guo G, Yang JL, Wei YQ, Qian ZY. In vitro drug release behavior from a novel thermosensitive composite hydrogel based on Pluronic f127 and poly (ethylene glycol)-poly (ε-caprolactone)-poly (ethylene glycol) copolymer. BMC biotechnology. 2009 Dec; 9(1):8.

Han L, Xu J, Lu X, Gan D, Wang Z, Wang K, Zhang H, Yuan H, Weng J. Biohybrid methacrylated gelatin/polyacrylamide hydrogels for cartilage repair. Journal of Materials Chemistry B. 2017; 5(4):731-41.

Heck T, Faccio G, Richter M, Thöny-Meyer L. Enzyme-catalyzed protein crosslinking. Applied microbiology and biotechnology. 2013 Jan 1; 97(2):461-75.

Hellio D, Djabourov M. Physically and chemically crosslinked gelatin gels. In Macromolecular Symposia 2006 Jul 1 (Vol. 241, No. 1, pp. 23-27). WILEY-VCH Verlag.

Hennink WE, van Nostrum CF. Novel crosslinking methods to design hydrogels. Advanced drug delivery reviews. 2012 Dec 1; 64:223-36.

Hoffman AS. Hydrogels for biomedical applications. Advanced drug delivery reviews. 2012 Dec 1; 64:18-23.

Homenick CM, de Silveira G, Sheardown H, Adronov A. Pluronics as crosslinking agents for collagen: novel amphiphilic hydrogels. Polymer International. 2011 Mar 1; 60(3):458-65.

Hospodiuk M, Dey M, Sosnoski D, Ozbolat IT. The bioink: A comprehensive review on bioprintable materials. Biotechnology advances. 2017 Apr 30; 35(2):217-39.

Jin R, Dijkstra PJ. Hydrogels for tissue engineering applications. InBiomedical applications of hydrogels handbook 2010 (pp. 203-225). Springer, New York, NY.

Johnson M. The Effect of Ultraviolet Light on Cell Viability, DNA Damage and Repair in Hutchinson-Gilford Progeria Syndrome and BJ Fibroblasts.

Jungst T, Smolan W, Schacht K, Scheibel T, Groll J. Strategies and molecular design criteria for 3D printable hydrogels. Chemical reviews. 2015 Oct 23; 116(3):1496-539.

Kamoun EA, Kenawy ER, Tamer TM, El-Meligy MA, Eldin MS. Poly (vinyl alcohol)-alginate physically crosslinked hydrogel membranes for wound dressing applications: characterization and bio-evaluation. Arabian Journal of Chemistry. 2015 Jan 1; 8(1):38-47.

Khattak SF, Bhatia SR, Roberts SC. Pluronic F127 as a cell encapsulation material: utilization of membrane-stabilizing agents. Tissue engineering. 2005 May 1; 11(5-6):974-83.

Lee KY, Mooney DJ. Alginate: properties and biomedical applications. Progress in polymer science. 2012 Jan 1; 37(1):106-26.

Lee VK, Lanzi AM, Ngo H, Yoo SS, Vincent PA, Dai G. Generation of multi-scale vascular network system within 3D hydrogel using 3D bio-printing technology. Cellular and molecular bioengineering. 2014 Sep 1; 7(3):460-72.

Li C, Faulkner-Jones A, Dun AR, Jin J, Chen P, Xing Y, Yang Z, Li Z, Shu W, Liu D, Duncan RR. Rapid formation of a supramolecular polypeptide–DNA hydrogel for in situ three-dimensional multilayer bioprinting. Angewandte Chemie International Edition. 2015 Mar 23; 54(13):3957-61.

Li X, Zhang J, Kawazoe N, Chen G. Fabrication of Highly Crosslinked Gelatin Hydrogel and Its Influence on Chondrocyte Proliferation and Phenotype. Polymers. 2017 Jul 26; 9(8):309.

Liang HC, Chang WH, Liang HF, Lee MH, Sung HW. Crosslinking structures of gelatin hydrogels crosslinked with genipin or a water-soluble carbodiimide. Journal of Applied Polymer Science. 2004 Mar 15; 91(6):4017-26.

Masutani EM, Kinoshita CK, Tanaka TT, Ellison AK, Yoza BA. Increasing thermal stability of gelatin by UV-induced cross-linking with glucose. International journal of biomaterials. 2014; 2014.

Mesa M, Sierra L, Patarin J, Guth JL. Morphology and porosity characteristics control of SBA-16 mesoporous silica. Effect of the triblock surfactant Pluronic F127 degradation during the synthesis. Solid State Sciences. 2005 Aug 1; 7(8):990-7.

Metters AT, Anseth KS, Bowman CN. Fundamental studies of a novel, biodegradable PEG-b-PLA hydrogel. Polymer. 2000 May 1; 41(11):3993-4004.

Michael S, Sorg H, Peck CT, Koch L, Deiwick A, Chichkov B, Vogt PM, Reimers K. Tissue engineered skin substitutes created by laser-assisted bioprinting form skin-like structures in the dorsal skin fold chamber in mice. PloS one. 2013 Mar 4; 8(3):e57741.

Nichol JW, Koshy ST, Bae H, Hwang CM, Yamanlar S, Khademhosseini A. Cell-laden microengineered gelatin methacrylate hydrogels. Biomaterials. 2010 Jul 1; 31(21):5536-44.

Nicodemus GD, Bryant SJ. Cell encapsulation in biodegradable hydrogels for tissue engineering applications. Tissue Engineering Part B: Reviews. 2008 Jun 1; 14(2):149-65.

Nie S, Hsiao WW, Pan W, Yang Z. Thermoreversible Pluronic® F127-based hydrogel containing liposomes for the controlled delivery of paclitaxel: in vitro drug release, cell cytotoxicity, and uptake studies. International journal of nanomedicine. 2011; 6:151.

Ouyang L, Yao R, Zhao Y, Sun W. Effect of bioink properties on printability and cell viability for 3D bioplotting of embryonic stem cells. Biofabrication. 2016 Sep 16; 8(3):035020.

Pereira RF, Bártolo PJ. 3D bioprinting of photocrosslinkable hydrogel constructs. Journal of Applied Polymer Science. 2015 Dec 20; 132(48).

Phelps EA, Enemchukwu NO, Fiore VF, Sy JC, Murthy N, Sulchek TA, Barker TH, García AJ. Maleimide cross-linked bioactive peg hydrogel exhibits improved reaction kinetics and cross-linking for cell encapsulation and in situ delivery. Advanced materials. 2012 Jan 3; 24(1):64-70.

Rajan N, Habermehl J, Coté MF, Doillon CJ, Mantovani D. Preparation of ready-to-use, storable and reconstituted type I collagen from rat tail tendon for tissue engineering applications. Nature protocols. 2006 Dec; 1(6):2753.

Refojo MF, Yasuda H. Hydrogels from 2-hydroxyethyl methacrylate and propylene glycol monoacrylate. Journal of Applied Polymer Science. 1965 Jul 1; 9(7):2425-35.

Resmi R, Unnikrishnan S, Krishnan LK, Kalliyana Krishnan V. Synthesis and characterization of silver nanoparticle incorporated gelatin‐hydroxypropyl methacrylate hydrogels for wound dressing applications. Journal of Applied Polymer Science. 2017 Mar 10; 134(10).

Rutz AL, Lewis PL, Shah RN. Toward next-generation bioinks: Tuning material properties pre-and post-printing to optimize cell viability. MRS Bulletin. 2017 Aug; 42(8):563-70.

Sakai S, Hirose K, Taguchi K, Ogushi Y, Kawakami K. An injectable, in situ enzymatically gellable, gelatin derivative for drug delivery and tissue engineering. Biomaterials. 2009 Jul 1; 30(20):3371-7.

Sarac AS. Redox polymerization. Progress in Polymer Science. 1999 Oct 1; 24(8):1149-204.

Shi W, He R, Liu Y. 3D printing scaffolds with hydrogel materials for biomedical applications. European Journal of BioMedical Research. 2015 Nov 4; 1(3):3-8.

Shikanov A, Zhang Z, Xu M, Smith RM, Rajan A, Woodruff TK, Shea LD. Fibrin encapsulation and vascular endothelial growth factor delivery promotes ovarian graft survival in mice. Tissue engineering part A. 2011 Sep 21; 17(23-24):3095-104.

Shoichet MS, Li RH, White ML, Winn SR. Stability of hydrogels used in cell encapsulation: An in vitro comparison of alginate and agarose. Biotechnology and bioengineering. 1996 May 20; 50(4):374-81.

Skardal A, Mack D, Kapetanovic E, Atala A, Jackson JD, Yoo J, Soker S. Bioprinted amniotic fluid-derived stem cells accelerate healing of large skin wounds. Stem cells translational medicine. 2012 Nov 1; 1(11):792-802.

Smith CM, Stone AL, Parkhill RL, Stewart RL, Simpkins MW, Kachurin AM, Warren WL, Williams SK. Three-dimensional bioassembly tool for generating viable tissue-engineered constructs. Tissue engineering. 2004 Sep 1; 10(9-10):1566-76.

Tan Y, Richards DJ, Trusk TC, Visconti RP, Yost MJ, Kindy MS, Drake CJ, Argraves WS, Markwald RR, Mei Y. 3D printing facilitated scaffold-free tissue unit fabrication. Biofabrication. 2014 Apr 10; 6(2):024111.

Thakur S, Govender PP, Mamo MA, Tamulevicius S, Thakur VK. Recent progress in gelatin hydrogel nanocomposites for water purification and beyond. Vacuum. 2017 Dec 1; 146:396-408.

Thomas BH, Fryman JC, Liu K, Mason J. Hydrophilic–hydrophobic hydrogels for cartilage replacement. Journal of the mechanical behavior of biomedical materials. 2009 Dec 1; 2(6):588-95.

Tibbitt MW, Anseth KS. Hydrogels as extracellular matrix mimics for 3D cell culture. Biotechnology and bioengineering. 2009 Jul 1; 103(4):655-63.

Van Den Bulcke AI, Bogdanov B, De Rooze N, Schacht EH, Cornelissen M, Berghmans H. Structural and rheological properties of methacrylamide modified gelatin hydrogels. Biomacromolecules. 2000 Mar 14;1(1):31-8.

Vashi AV, Keramidaris E, Abberton KM, Morrison WA, Wilson JL, O'Connor AJ, Cooper-White JJ, Thompson EW. Adipose differentiation of bone marrow-derived mesenchymal stem cells using Pluronic F-127 hydrogel in vitro. Biomaterials. 2008 Feb 1; 29(5):573-9.

Wang H, Zhou L, Liao J, Tan Y, Ouyang K, Ning C, Ni G, Tan G. Cell-laden photocrosslinked GelMA–DexMA copolymer hydrogels with tunable mechanical properties for tissue engineering. Journal of Materials Science: Materials in Medicine. 2014 Sep 1; 25(9):2173-83.

Wang X, Yan Y, Pan Y, Xiong Z, Liu H, Cheng J, Liu F, Lin F, Wu R, Zhang R, Lu Q. Generation of three-dimensional hepatocyte/gelatin structures with rapid prototyping system. Tissue engineering. 2006 Jan 1; 12(1):83-90.

White CJ, McBride MK, Pate KM, Tieppo A, Byrne ME. Extended release of high molecular weight hydroxypropyl methylcellulose from molecularly imprinted, extended wear silicone hydrogel contact lenses. Biomaterials. 2011 Aug 1; 32(24):5698-705.

Xavier JR, Thakur T, Desai P, Jaiswal MK, Sears N, Cosgriff-Hernandez E, Kaunas R, Gaharwar AK. Bioactive nanoengineered hydrogels for bone tissue engineering: a growth-factor-free approach. ACS nano. 2015 Feb 25; 9(3):3109-18.

Xu W, Wang X, Yan Y, Zheng W, Xiong Z, Lin F, Wu R, Zhang R. Rapid prototyping three-dimensional cell/gelatin/fibrinogen constructs for medical regeneration. Journal of bioactive and compatible polymers. 2007 Jul; 22(4):363-77.

Yamamoto M, James D, Li H, Butler J, Rafii S, Rabbany S. Generation of stable co-cultures of vascular cells in a honeycomb alginate scaffold. Tissue Engineering Part A. 2009 Oct 7; 16(1):299-308.

Yanez M, Rincon J, Dones A, De Maria C, Gonzales R, Boland T. In vivo assessment of printed microvasculature in a bilayer skin graft to treat full-thickness wounds. Tissue Engineering Part A. 2014 Aug 28; 21(1-2):224-33.

Ye Q, Zünd G, Benedikt P, Jockenhoevel S, Hoerstrup SP, Sakyama S, Hubbell JA, Turina M. Fibrin gel as a three dimensional matrix in cardiovascular tissue engineering. European Journal of Cardio-Thoracic Surgery. 2000 May 1; 17(5):587-91.

Yin J, Yan M, Wang Y, Fu J, Suo H. 3D Bioprinting of Low-Concentration Cell-Laden Gelatin Methacrylate (GelMA) Bioinks with a Two-Step Cross-linking Strategy. ACS applied materials & interfaces. 2018 Feb 15; 10(8):6849-57.

Yue K, Trujillo-de Santiago G, Alvarez MM, Tamayol A, Annabi N, Khademhosseini A. Synthesis, properties, and biomedical applications of gelatin methacryloyl (GelMA) hydrogels. Biomaterials. 2015 Dec 31; 73:254-71.

Zhu J, Marchant RE. Design properties of hydrogel tissue-engineering scaffolds. Expert review of medical devices. 2011 Sep 1; 8(5):607-26.